Nickel sorption on calcite surface: a macroscopic experimental study

By

Thais R. LAMANA

Department of Earth and Planetary Sciences

McGill University, Montréal, Canada

November 2010

A thesis submitted to McGill University in partial fulfillment

of the degree of Master of Science.

Preface

As described on the thesis, e-thesis and non-thesis information section of the Graduate and Postdoctoral Studies Office (GPSO) guidelines of McGill University, the candidates have the option of including, as part of the thesis, the text of one or more papers submitted, or to be submitted, for publication. As manuscripts for publication are frequently very concise documents, where appropriate, additional material must be provided (e. g. in appendices) in sufficient detail to allow a clear and precise judgement to be made of the importance and originality of the research reported in the thesis. Accordingly, the thesis must include: a table of contents; a brief abstract in both English and French; an introduction which clearly states the rational and objectives of the research; a comprehensive review of the literature (in addition to that covered in the introduction to each paper); a final conclusion and summary and a thorough bibliography.

Hence, the first chapter of this thesis includes a general introduction about Nickel (Ni) biogeochemistry and a review of Ni adsorption studies carried out to date on common rock-forming minerals (e. g. calcite, oxides), and of the adsorption behaviour of divalent metal ions on calcite as well as the mechanisms involved in the process. The impetus of the study and research objectives are presented at the end of the first chapter. The second chapter is an integral version of a paper destined for publication in the Journal of Colloid and Interface Science. It contains a detailed description of the experimental work carried out to characterize the adsorption behaviour of Ni on calcite under controlled laboratory conditions and how the objectives previously established were achieved. In this chapter, the reader will find results of the experimental study and their interpretation. Finally, the third chapter summarizes the conclusions drawn from the

experimental results, along with recommendations for future work, specifically how to maximize the acquisition of data and Ni adsorption modelling capabilities.

Contribution of Authors

I, hereby, declare that all the laboratory and analytical work presented in this thesis was completed by myself. Dr. Prof. Alfonso Mucci provided guidance on the research methodology and advised me with the processing and interpretation of the data, as well as guaranteeing coherent scientific work throughout the project.

Dedication

- This thesis is dedicated to my parents (Chirley and Adilson), for their everlasting love, support, strength and faith in me since the beginning of my science studies.
- Portuguese translation: “Esta tese é inteiramente dedicada aos meus pais (Chirley e Adilson) pelo inesgotável amor, apoio, força e fé em mim desde o início de minha carreira científica.”
- I also would like to extend my dedication towards my beloved Paul, who constantly and patiently understood me throughout the years with much love and caress.

Acknowledgements

- My sincere gratitude goes to Dr. Alfonso Mucci for his mentorship, assistance, advice and editing efforts that were indispensable for the completion of this thesis. Additionally, I would like to thank him for the funding he provided towards the development of this research project.

- I would like to extend my gratitude to Dr. Jeanne Paquette for her time and advice in her capacity as supervisory committee member.

- I would like to thank the department laboratory staff; Glenna Keating and Isabelle Richer for their assistance in the geochemical laboratory, Constance Guignard (research associate) for her assistance with the general management of the low temperature geochemistry laboratory.

- I would like to thank my dear colleagues: Fatimah Sulu-Gambari, Dominique Richard, Qiang Chen and Stelly Lefort for their support and constructive advice throughout the course of my master's degree.

- I also wish to thank Anne Kosowski, Angela Di Ninno, Kristy Thornton and Brigitte Dionne for making the life of students more practical and pleasant at EPS.

Table of Contents

List of Figures

List of Tables

Abstract

In natural aqueous systems, adsorption and co-precipitation (sorption) are regarded as possible metal sequestration mechanisms that would promote *in situ* passive remediation. Calcite is a ubiquitous mineral on the Earth's surface, whose propensity to scavenge trace metals has been extensively investigated. Since Nickel (Ni) appears on the EPA "priority list" of pollutants, identifying factors that may control its fate in calcite-rich natural waters (e.g. groundwaters, carbonate-rich coastal and marine sediments) is critical. Unfortunately, scarce literature is dedicated to the influence of mineral properties and solution chemistry on the affinity and sorption mechanisms of Ni on the calcite surface. With that in mind, batch sorption experiments were conducted, under controlled laboratory conditions (ambient temperature of 25 ± 2ºC, and atmospheric $pCO_2 = 10^{-3.41}$atm) in calcite-saturated 0.1M and 0.7M NaCl solutions over a range of pH (7.5 to 8.9) and total Ni concentrations- $[Ni]_{total}$- (1.2×10^{-4} to 3.5×10^{-6} M), to characterize the affinity of Ni for the calcite surface. Our experimental results revealed that the first 24 hours of reaction are critical to the metal-mineral interaction and the fractional Ni(II) sorption varied with solution pH and Ni(II) aqueous speciation. Notably, Ni sorption onto the calcite surface increased with pH and was well correlated to the relative abundance of the $NiCO_3^0{}_{(aq)}$ species (ion-pair) over the pH range studied. After 24 hours, the overall Ni fractional sorption was attenuated with an increase of the background electrolyte (NaCl) concentration. The application of adsorption isotherm models (Langmuir and Freundlich) allowed us to highlight the dependence of adsorption to the $[Ni]_{total}$ and solution pH. Finally, irrespective of the solution ionic strength (0.1 and 0.7 M NaCl), Ni did not desorb readily when the total Ni(II) concentration in solution exceeded 4.0×10^{-5}M.

Résumé

Dans les systèmes aquatiques naturels, l'adsorption et la co-précipitation (sorption) sont considérés comme des processus passifs de séquestration *in-situ* des métaux lourds. La calcite est un minéral très abondant dans la croûte terrestre et un puits pour plusieurs métaux. Par conséquent, sa capacité de séquestration de métaux a été largement étudiée. Puisque le nickel (Ni) est considéré comme un polluant dangereux pour la santé humaine et environnementale, l'identification des facteurs qui peuvent contrôler son devenir dans les milieux naturels riches en calcite (eaux souterraines riches en carbonate ou sédiments côtiers et marins) est essentielle. Malheureusement, il y a peu de littérature pertinente sur l'influence des propriétés du minéral et la composition de la solution sur l'affinité et les mécanismes de sorption du Ni(II) à la surface de la calcite. Vu le manque d'information sur le sujet, nous avons mené une étude sous des conditions contrôlées en laboratoire (température ambiante de 25 (±2°C) et une pression partielle de $CO_2 = 10^{-3.41}$atm) dans des solutions aqueuses de NaCl saturées en calcite. Afin de caractériser l'affinité du Ni(II) pour la surface de la calcite, les expériences ont été effectuées dans des solutions de force ionique (0.1M et 0.7M), pH et concentration totale de Ni ($[Ni]_{total}$) variées. Les résultats révèlent que les 24 premières heures de réaction sont critiques pour la sorption du Ni(II). La sorption du Ni(II) sur la calcite augmente avec le pH de la solution mais diminue avec l'augmentation de la concentration de NaCl. Indépendamment de la force ionique, la sorption fractionnelle du Ni est fortement corrélée avec l'abondance relative du complexe $NiCO_3^o{}_{(aq)}$ dans l'intervalle de pH étudié. Quelle que soit la force ionique (0.1M et 0.7M NaCl) de la solution, le Ni(II) ne se désorbe pas suite à son adsorption dans les solutions dont la concentration totale en Ni est supérieure à 4.0×10^{-5}M.

Chapter 1- Introduction and literature review

1.1 -Introduction

Nickel (Ni) is an important element in the modern industry; by far its largest use is for the manufacture of stainless steel. Laterite and sulfide Ni deposits are the major sources of economic Ni ores (Dalvi *et al*., 2004). Canada (sulfidic Ni/Cu-ores at the Sudbury and Thompson mines) is the second largest producer of Ni in the world, with an annual production of approximately 197,000 tonnes (Canadian Environmental Protection Act. 1994). The increasing demand for Ni-containing products inevitably leads to an increase in the discharge of Ni-rich by-products and wastewaters into the environment, deteriorating air, soil and water quality (Denkhaus and Salnikow, 2002). Hence, in order to manage public health, environmental and health agencies (e.g. U.S. EPA, Environment and Health Canada) elaborated drinking water quality criteria regarding the presence of harmful heavy metals (e.g., Ni).

Wastewaters and Ni-rich atmospheric fallout derived from mines operations, smelters, refineries and the incineration of urban wastes contribute to the Ni load of natural bodies of water. Natural background Ni concentrations in aquatic systems range from 0.2 ppb (~10^{-9} M) to 0.7 ppb (~$1.1x10^{-8}$ M) in the open ocean to approximately 2 ppb (~$3.4x10^{-8}$ M) in freshwaters (e.g. lakes and streams) (Nieminen *et al.,* 2007[1]). Nevertheless, the estimated total loading of Ni to water in Canada in both 1988 and 1990 from mining, smelting, and refinery operations was estimated at 64 tons, with dissolved Ni concentrations in these effluents ranging from 16 to 27,200 ppm (~2.7×10^{-4} - 0.45 M) (Canadian Environmental Protection Act. 1994). Since then, upon the implementation of

government regulations (e.g. the shutdown of smelters, dispersion and reduction of emissions), improvements have been made to drastically reduce Ni's effluent waste concentrations and atmospheric emissions (Hutchinson and Havas, 1986). Unfortunately, lakes (Hannah and Crooked) within the Sudbury district in Ontario remain contaminated with Ni, with dissolved concentrations exceeding 100 ppb (1.7×10^{-6} M), well above the threshold value of 50 ppb (0.85×10^{-6} M) set for drinking water by Health Canada (Ponton and Hare, 2009).

The total concentration of a metal in any system, environment or human, is not necessarily a good indicator of its potential health impact. The toxicity of a metal ion is contingent upon its speciation under a set of environmental conditions (e.g., pH, Eh). Oxidation state, coordination (including the number and type of ligands), and physical state or association with other phases contribute to define speciation (Reeder *et al.,* 2006). Over the pH range of most natural waters, Ni^{2+} is the only stable oxidation state, although, in increasingly calcareous/alkaline waters, the following complexes; $NiHCO_3^-$, $NiCO_3^0$ and $Ni(OH)_2^0$ may be stable (Fig. 1.1) (Nieminen *et al.,* 2007). Chronic exposure to Ni compounds can have adverse effects on human health. For instance, Ni allergy, in the form of contact dermatitis, is the most common and well-known type of reaction. Additionally, epidemiological studies have clearly implicated Ni compounds as a human carcinogen, based upon a higher incidence of lung and nasal cancer among Ni mining, smelting and refinery workers. For this reason, the International Agency for Research on Cancer (IARC) has classified all Ni compounds, except the Ni^0 (metallic Ni), as cancerogens to humans (Denkhaus and Salnikow, 2002).

Since Ni-contaminated water poses a major environmental and human health problem, Ni-rich effluents should be prevented from reaching natural bodies of water.

Furthermore, natural waters (ground and surface) that are already impacted by metal contamination should be or are being remediated to reinstate the sustainability of these systems (Kukier and Chaney, 2004). There are many proven active remediation processes and technologies that can be employed in the management of contaminated sites. Nevertheless, no single technology/process is universally applicable with equal success to all contaminant types at all sites and many are costly and unsustainable (Asante-Duah, 1996). On the other hand, passive remediation relies on natural processes, such as biological and/or chemical processes, that sequester and/or transform contaminants in the system. The latter may require more time to achieve acceptable levels of contamination but they may significantly reduce the cost of remediation (Gambolati and Verri, 1995).

An important consideration of a passive remediation approach of Ni-contaminated sites should be whether the surrounding matrix acquires components that are naturally capable of reducing its concentration and mobility within the aqueous system (Suthersan, 2001). In natural aquatic systems, the sequestration of contaminants (e.g., Ni) is mediated by geochemical processes, which inherently involve mineral-water interactions and where sorption is by far the most studied phenomena (Reeder *et al.,* 2006). Sorption is essentially defined as a surface retention process, irrespective of its mechanism (Sposito, 1986), often implied to include both adsorption and co-precipitation processes (Sposito, 1984; Zachara, 1991). Adsorption refers to a surface-limited (or 2-D) process, where there is interfacial accumulation of a given adsorbate (e.g., metal cations) whereas co-precipitation occurs when a contaminant is incorporated in the bulk solid – a 3-D process - and removed from the environment until the host phase is dissolved (Roman-Ross *et al.,* 2006).

Adsorption and co-precipitation techniques, using natural minerals, are becoming popular in heavy-metal-removal water treatment systems because of their low maintenance cost, simple design, and ease of operation (Sharma *et al.,* 1990). Sharma *et al.* (1990) performed an experimental study (at 30°C) that successfully removed 92% of total Ni from aqueous solution in two hours using 20 g L^{-1} of wollastonite (α-$CaSiO_3$, a clay mineral) as an adsorbent. The removal of Ni increased from 10 to 92% as pH was increased from 3.0 to 8.0, but the Ni uptake remained almost unchanged at higher pHs. Moreover, in a comparative study (at 25°C, $pCO_2= 10^{-3.5}$ atm, solid:solution ratio ranging from 4 mg L^{-1} to 400 mg L^{-1} and $[Ni]_{total} = 6.8x10^{-5}$ M to $4.0x10^{-4}$ M) with five different solid surfaces (calcite, humic acid, montmorillonite, and iron and manganese oxy-hydroxides), Pedersen-Green *et al.* (1997) demonstrated that the adsorption capacity of oxy-hydroxides of manganese (MnO_2) and iron ($Fe(OH)_3$) (at pH 6.7-8.4) was much larger than the other solid phases considered, keeping the Ni dissolved concentrations well below the Danish drinking water threshold value of 50 ppb. Until now, many of these studies have been carried out to develop new technological schemes of safe heavy metal waste storage, although they require that the affinity of metal cations, such as Ni(II), for various mineral surfaces be investigated under a variety of environmental conditions. Optimally, these minerals should be readily available and inexpensive.

Carbonates are an important group of minerals that are ubiquitous in the Earth's crust and critical components in both marine and fresh water environments (Morse *et al.*, 2007). Of rock-forming carbonates, calcite ($CaCO_3$) and dolomite ($CaMg(CO_3)_2$) are the most abundant minerals, accounting for more than 90% of natural carbonates (Reeder, 1983). Calcite is the thermodynamically stable polymorph of calcium carbonate minerals under earth surface conditions (Morse and Mackenzie, 1990). Due to its reactivity,

calcite plays a critical role in the chemistry of natural aqueous solutions, regulating their pH and alkalinity by means of dissolution and precipitation (Morse *et al*., 2007). Furthermore, via sorption reactions, calcite may affect the mobility and geochemical cycling of trace metals in aquatic environments (Van Cappellen et al. 1993; Martin-Garin *et al.* 2003; Villegas-Jimenez, 2009). More importantly, it may serve as a potentially significant metal-scavenging mineral in water and soil environments as well as in waste systems (Sanchez and Alvarez-Ayuso, 2002). For instance, Wang and Reardon (2001) demonstrated the effectiveness of a mixture of siderite ($FeCO_3$) and limestone ($CaCO_3$) to remove cadmium (Cd) and arsenic (As) from mining wastewaters.

1.2- Literature review

1.2.1-Adsorption behaviour of divalent metal ions on calcite

A great deal of information has been gathered about the sorption properties of calcite, especially its propensity to uptake divalent cations (Davis et al. 1987; Zachara *et al.* 1991; Green-Pedersen *et al.* 1997; Lakshtanov and Stipp, 2007). Foremost, Zachara *et al.* (1991) studied the sorption behaviour of seven different divalent metal cations (Ba, Sr, Cd, Mn, Co and Ni) in calcite-saturated solutions under ambient conditions (~ 25ºC and atmospheric $pCO_{2(g)}=10^{-3.5}$). They present metal adsorption as an ion exchange reaction with Ca ions (eq.1) exposed on a calcite surface ($>Ca^+$) or by the metal complexation to carbonate groups ($>CO_3^-$) on a hydrated surface layer (because the Ca^{2+} and CO_3^{2-} charges are partially satisfied by coordination to the underlying bulk crystal).

$$>Ca^- + Me^{2+}_{(aq)} = >Me^+ + Ca^{2+}_{(aq)} \qquad (1)$$

Basically, their interpretation of metal adsorption relied on the fact that, among the metals studied, those with ionic radii smaller than Ca^{2+} (Table 1.1) were more strongly adsorbed to the calcite surface. Additionally, the fractional metal adsorption (Fig. 1.2) consistently decreased with increasing difference between the Ca^{2+} and Me^{2+} ionic radii (Table 1.1). Nevertheless, Mn and Zn showed a reverse affinity with respect to this trend (Fig. 1.2). The authors concluded that, for many of the metals studied, the magnitude of sorption on calcite was sufficiently large that calcite could act as an important sorbent for the removal of those metals in calcite-rich environments. Ni, Ba, Sr were considered as exceptions and the effectiveness of their removal by the calcite surface was questioned by the authors.

Nevertheless, it is important to note that the efficiency of sorption is contingent upon the physical (e.g. temperature, sorbent particle loading) and chemical properties (e.g. pH, ionic strength) of the system which, when altered, can either reduce or promote metal sorption (Rouff *et al.* 2005). For this reason, a number of laboratory-based studies have traditionally focused on "batch sorption experiments" whereby the influence of variables such as pH, $pCO_{2(g)}$, metal concentration, ionic strength, background electrolyte (nature and concentration), surface area and time, on the sorption processes were examined (Jenne, 1998; Rouff *et al.,* 2002). In calcite-saturated systems, the solution pH has been the most widely investigated parameter because it exerts a major influence on the dissolved metal (Fig.1) and calcite surface speciation, Ca^{2+} aqueous concentration (activity) and mineral surface charge (pHznpc). The adsorption of divalent metals on calcite is considered to be strongly pH-dependent (Davis *et al.,* 1987; Zachara *et al.,* 1991; Rouff *et al.,* 2005). For instance, free metal cations compete directly with Ca^{2+} (or other cationic species in solution) for the adsorption surface sites. Zachara *et al.* (1991)

observed an increase of the fractional sorption of all the divalent metals studied as pH was increased (Fig.2). Other experimental studies have corroborated these findings for the same (Stipp *et al.* 1992; Belova *et al.* 2008) as well as other divalent metal cations (e.g., Pb^{2+}) (Rouff *et al.,* 2002, 2005).

Additionally, the formation of metal-ligand complexes in solution has been observed to significantly influence the metal uptake by calcite (Rouff *et al.,* 2005). For instance, Van der Weijden and Comans (1997) demonstrated that the presence of phosphate (PO_4^{3}; 10^{-9} to 10^{-4}M) and sulfate (SO_4^{-2}; 10^{-5} to 10^{-1}M) in solution reduced the cadmium (Cd^{2+}) fractional sorption on calcite. The reduced Cd^{2+} uptake by calcite from sulfate-rich solutions was also attributed to Cd-sulfate complexation. Similarly, Rouff and co-workers (2005) reported a systematic decrease in Pb sorption on calcite with increasing chloride concentrations. They proposed that the formation of Pb-chloro complexes decreases the amount of Pb^{2+} available for sorption.

1.2.2-Calcite surface and metal adsorption mechanisms

It is reasonable to state that the chemical composition of an aqueous solution is key to predict the affinity of divalent metal cations for the calcite surface. Provided that conditions do not induce the precipitation a distinct adsorbate (e.g., divalent heavy metal cation) solid-phase, its uptake from the aqueous solution by calcite can readily be described by experiment-accessible quantities (e.g., adsorption isotherms and partition coefficients) that solely provide a macroscopic interpretation of what is happening at the solution-solid interface (Villegas-Jimenez *et al*, 2009). Accordingly, with regards to adsorption reactions, conceptual models (e.g. Langmuir and Freundlich models) are

commonly used to represent the interactions between the adsorbate and the mineral particle surface. For instance, one of the Langmuir model assumptions requires a 1:1 stoichiometry (eq.2) which imposes that one adsorption site binds to a single adsorbate until the attainment of equilibrium and the formation of a monolayer. This model does not discriminate between surface sites and, hence, the energy of the interaction does not change with the adsorption density (e.g. amount adsorbed per m^2). Based on the mass action law (eq.2), it is possible to derive the reaction constant (K_{ads}) (eq.4) and the maximum adsorption capacity (S_{Tmax}; eq.3) which is limited by the number of sites (Honeyman and Leckie, 1986; Stumm and Morgan 1996) at the imposed conditions. On the other hand, the Freundlich model is often applied to describe adsorption onto heterogeneous surfaces where the saturation of adsorption sites is never attained because the formation of a multi-layer is possible. Thus, adsorption is described by the Freundlich constant (*m*) along with a measure of non-linearity (*n*) of the data set. In both models, the descriptions of adsorbate-solid interactions are based on net changes of the aqueous phase adsorbate concentration (activity). Notwithstanding, they do not explicitly identify the details of such interactions (Honeyman and Leckie, 1986).

$$\mathbf{>S + A_{(aq)} \leftrightarrow >SA} \qquad (2)$$

$$\mathbf{S_{Tmax} = >S + >SA} \qquad (3)$$

$$\mathbf{Kads = [>SA]/\ [>S]*[A_{(aq)}]} \qquad (4)$$

where:

>S = mineral surface site

$A_{(aq)}$ = adsorbate in solution

>SA = adsorbate bound to the surface site

S_{Tmax} = maximum adsorption capacity

Nevertheless, there have been recent developments of mathematical models and high resolution microscopic techniques to describe the calcite surface behaviour in aqueous solutions, particularly in relation to the adsorption, desorption and co-precipitation of foreign ions (Van Cappellen *et al.* 1993; Stipp, 1999). These models originate from surface complexation theory which describes chemical surface reactions in terms of speciation at the solid-solution interface. These surface complexation models (SCMs) are based on mass law equations that may serve as a framework for the prediction of adsorption in any given system, upon the development of a proper thermodynamic database (Stumm and Morgan, 1996; Pokrovsky and Schott, 2002; Villegas-Jimenez *et al.*, 2009).

The SCMs (Table 1.2) for the metal-carbonate/solution interface (Van Cappellen et al. 1993, Pokrovsky et al. 2000, Pokrovsky and Schott, 2002) postulate the formation of two primary hydration sites on the mineral surface; $>MeOH^0$ and $>CO_3H^0$ (where Me indicates the metal cation). In these models, the surface sites exposed upon cleavage are assigned +1 and -1 charges (as stated previously, Ca^{2+} and CO_3^{2-} charges are partially satisfied by coordination to the underlying bulk crystal). Depending on pH, subsequent hydration and adsorption of constituent ions from solution lead to the formation of the following surface species: $>CO_3^-$, $>CO_3Me^+$, $>MeO^-$, $>MeOH_2^+$, $>MeHCO_3^0$ and $>MeCO_3^-$ (Pokrovsky *et al.* 2000). As a result of the calcite amphoteric (acid-base) behaviour, it is likely that protonated carbonate surface groups ($>CO_3H^0$) dominate in acid solutions, and hydrated calcium groups ($>CaOH_2^+$) in neutral-alkaline solutions (Pokrovsky and Schott, 2002). Hence, given an understanding of factors that control

calcite surface speciation, it is possible to better predict how its surface electrical properties may affect metal adsorption. The increased metal adsorption with increasing pH is related to the overall surface charge of the calcite particle. The calcite surface electrical charge develops in response to the adsorption of "potential determining ions ($PDI_{(s)}$)", such as H^+, OH^- and other charged ions on the mineral surface (e.g. Ca^{2+}, CO_3^{2}-, HCO_3^-). For instance, the point of zero charge on a mineral's surface corresponds to the pH value (pH_{pzc}) where the net surface charge is zero. If the surface charge is established solely by the adsorption of H^+ and OH^-, one may also refer to the point of zero net proton charge (pH_{pznpc}) (Stumm and Morgan, 1996). A net positive or negative surface charge induces the migration of oppositely-charged ions in solution towards the surface (Moulin and Roques, 2003). The metal ion may adsorb as an outer-sphere or inner-sphere complex, depending on whether the interaction is electrostatic or chemical (e.g. covalent or ionic) respectively (Stumm and Morgan, 1996).

1.3-Impetus of the study

Ni is considered a priority pollutant in accordance with the USEPA "Red List". Although many factors may control its fate in calcite-rich natural waters (e.g. groundwaters, carbonate-rich coastal and marine sediments), there is a scarcity of literature dedicated to the sorption behaviour and interactions between Ni and calcite. Thus, relationships between its sorption behaviour, calcite surface properties, and solution chemistry have not yet been established. Furthermore, a single publication (Zachara *et al.* 1991) reports, to a limited extent, on Ni sorption reversibility on calcite.

1.4- Research objectives

To provide new insights about factors that promote or inhibit Ni uptake by calcite in $CaCO_3$-saturated natural aquatic systems, the present study aims to:

- Explore the influence of background electrolyte (NaCl), pH, ionic strength, Ni concentration, and reaction times on the uptake of this metal by the calcite surface.
- Describe Ni adsorption in terms of isotherm models (Langmuir and Freundlich), in order to derive mass action relationships (K_{ads}).
- Provide novel information about the desorption behaviour Ni under various conditions (e.g., pH, ionic strength and total Ni concentration).

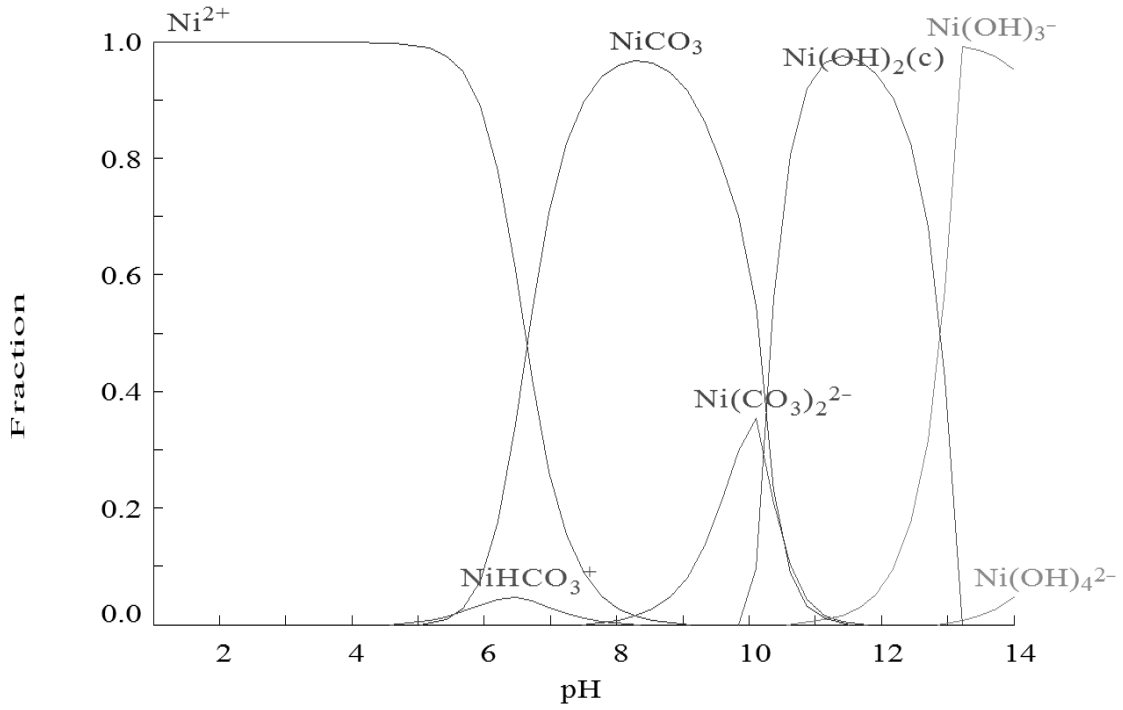

Figure 1.1 - Simulation of nickel species distribution in a calcareous environment as a function of pH. This calculation was based on the following solution composition: [Ni]total=10^{-7}M, $CaCO_3$-saturated, ionic strength equivalent to 1.5 x10^{-3} M at 25ºC and 1 atm total pressure ($pCO_{2(g)}$=$10^{-3.41}$ atm) (Puigdomenech, 2002).

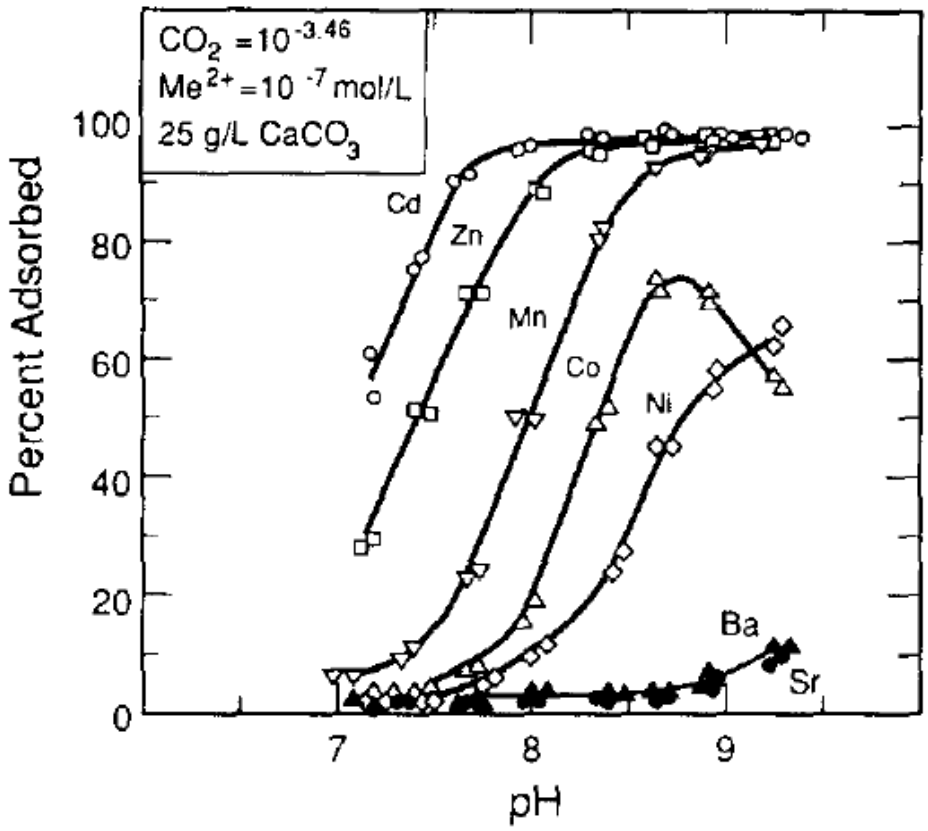

Figure1.2- Fractional sorption of divalent metals on calcite as a function of pH, in a calcite-saturated solution in equilibrium with atmospheric $pCO_{2(g)}$. With the exception of Co which precipitates as $Co(OH)_2$ at high pHs, the fractional adsorption of each metal increases with increasing pH until saturation of the surface. (Zachara *et al.* 1991)

Table.1.1- Divalent metal ion properties, including their ionic radius and size disparity relative to Ca (Δradius). $\Delta G°_H$ are the standard single-ion Gibbs free energies of hydration. Modified from Table 1 of Zachara *et al.* (1991).

Metal	radius size (Å)	Δ radius (Me_{radius}-Ca_{radius}) (Å)	ΔG_H (KJ/mol)
Ba (Barium)	1.34	0.35	-1318.53
Sr (Strontium)	1.12	0.13	-1447.41
Ca (Calcium)	0.99	0	-1593.45
Cd (Cadmium)	0.97	-0.02	-1801.42
Mn (Manganese)	0.80	-0.19	-1831.97
Zn (Zinc)	0.74	-0.25	-2027.80
Co (Cobalt)	0.72	-0.27	-2006.46
Ni (Nickel)	0.69	-0.30	-2067.97

Table1.2-Surface complexation reactions and their intrinsic stability constants (log $K°_{int}$) at the calcite/solution interface at 25°C and $pCO_2 = 10^{-3.5}$atm (Pokrovsky and Scott, 2002).

Surface Reaction	log $K°_{int}$ (I= 0 M)
$>CO_3H^0 = >CO_3^- + H^+$	-5.1
$>CO_3H^0 + Ca^{2+} = > CO_3Me^+ + H^+$	-1.7
$>CaOH^0 - H^+ = >CaO^-$	-12
$>CaOH^0 + H^+ = >CaOH_2^+$	11.85
$>CaOH^0 + CO_3^{2-} + 2H+ = >CaHCO_3^0 + H_2O$	23.5
$>CaOH^0 + CO_3^{2-} + H+ = >CaCO_3^- + H_2O$	17.1

1.5-References

Asante-Duah, D. K. (1996). Managing Contaminated Sites: Problem Diagnosis and Development of Site Restoration. New York, John Wiley. 410 pp.

Belova, D. A., Lakshtanov, L. Z., *et al.* (2008). Experimental study of Ni adsorption on chalk: preliminary results. Mineral Magazine **72**(1): 377-379.

Canadian Environmental Protection Act. Government of Canada (1994). Nickel and its compounds. In: Priority Substances List Assessment Report. Environment Canada and Health Canada. Ottawa, Ministry of Supply and Services. 89 pp.

Dalvi, A.D., Gordon-Bacon, W., *et al.* (2004). The Past and the Future of Nickel Laterites. PDAC International convention. Trade Show and Investors Exchange. Toronto, March 7-10, 2004.

Davis, J. A., Fuller, C. C. *et al.* (1987). A model for trace metal sorption processes at the calcite surface: Adsorption of Cd^{2+} and subsequent solid solution formation. Geochimica et Cosmochimica Acta **51**(6): 1477-1490.

Denkhaus, E. and Salnikow, K. (2002). Nickel essentiality, toxicity, and carcinogenicity. Critical Reviews in Oncology/Hematology **42**(1): 35-56.

Gambolati G. and Verri. G. (1995). Advanced methods for groundwater pollution control. CISM- Courses and Lectures **364**. New York, Springer-Verlag. 288 pp.

García-Sánchez, A. and Álvarez-Ayuso, E. (2002). Sorption of Zn, Cd and Cr on calcite. Application to purification of industrial wastewaters. Minerals Engineering **15**(7): 539-547.

Green-Pedersen, H., Jensen, B. T., *et al.* (1997). Nickel adsorption on MnO_2, $Fe(OH)_3$, montmorillonite, humic acid and calcite: a comparative study. Environmental Technology **18**: 807-815.

Honeyman B.D. and Leckie, O. J. (1986). Macroscopic partitioning coefficients for metal ion adsorption. In: Davis, J. A. and Hayes, K. F., (Editors). Geochemical Processes at Mineral Surfaces. Washington, D.C, American Chemical Society **323:** 162-190.

Hutchinson, T. and Havas, M. (1986). Recovery of previously acidified lakes near Coniston, Canada, following reductions in atmospheric sulfur and metals emissions. Water, Air and Soil Pollution **28:** 319-333.

Jenne, E. A. (1998). Adsorption of metals by geomedia: data analysis, modeling, controlling factors, and related issues. In: Jenne, E. A., (Editor). Adsorption of Metals by Geomedia. San Diego, Academic Press**:** 1-73.

Kukier, U. and Chaney, R. L. (2004). *In Situ* remediation of nickel phytotoxicity for different plant species. Journal of Plant Nutrition **27**(3): 465 - 495.

Lakshtanov, L. Z. and Stipp, S. L. S. (2007). Experimental study of nickel(II) interaction with calcite: Adsorption and co-precipitation. Geochimica et Cosmochimica Acta **71**(15): 3686-3697.

Martin-Garin, A., Van Cappellen, P., *et al.* (2003). Aqueous cadmium uptake by calcite: a stirred flow-through reactor study. Geochimica et Cosmochimica Acta **67**(15): 2763-2774.

Morse, J.W. and Mackenzie, F.T. (1990). Geochemistry of sedimentary carbonates. In: Developments in Sedimentology **48.** New York, Elsevier. 707 pp.

Morse, J. W., Arvidson, R. S., *et al.* (2007). Calcium carbonate formation and dissolution. Chemical Reviews **107**(2): 342-381.

Moulin, P. and Roques, H. (2003). Zeta potential measurement of calcium carbonate. Journal of Colloid and Interface Science **261**(1): 115-126.

Nieminen, T.M., Ukonmaanaho, L., *et al*. (2007) Biogeochemistry of Nickel and its release into the environment. In: Sigel, A.; Sigel, H. and Sigel, R. K. O., (Editors). Metal Ions in Life Sciences. New York, Wiley. **2:** 1–30.

Pokrovsky, O. S. and Schott, J. (2002). Surface chemistry and dissolution kinetics of divalent metal carbonates. Environmental Science & Technology **36**(3): 426-432.

Pokrovsky, O. S., Mielczarski, J. A., *et al.* (2000). Surface speciation models of calcite and dolomite/aqueous solution interfaces and their spectroscopic evaluation. Langmuir **16**(6): 2677-2688.

Ponton, D. E. and Hare, L. (2009). Assessment of Nickel contamination in lakes using the phantom midge *Chaoborus* as a biomonitor. Environmental Science & Technology **43**(17): 6529-6534.

Puigdomenech, I. (2002). HYDRA MEDUSA, make equilibrium diagrams using sophisticated algorithms. Royal Institute of Technology; Stockholm, Sweden.

Reeder, R. J. (1983). Crystal chemistry of the rhombohedral carbonates. In: Reeder, R. J., (Editor). Carbonates: Mineralogy and Chemistry. Reviews in Mineralogy. Washington, Mineralogical Society of America **2:** 1-48.

Reeder, R. J., Schoonen, M. A. A., *et al.* (2006). Metal speciation and its role in bioaccessibility and bioavailability. Reviews in Mineralogy and Geochemistry **64**(1): 59-113.

Román-Ross, G., Cuello, G. J., *et al.* (2006). Arsenite sorption and co-precipitation with calcite. Chemical Geology **233**(3-4): 328-336.

Rouff, A., Reeder, R., *et al.* (2002). Pb (II) Sorption with calcite: a radiotracer study. Aquatic Geochemistry **8**(4): 203-228.

Rouff, A. A., Reeder, R. J., *et al.* (2005). Electrolyte and pH effects on Pb(II)-calcite sorption processes: the role of the $PbCO_3^0$(aq) complex. Journal of Colloid and Interface Science **286**(1): 61-67.

Sharma, Y. C., Gupta, G. S., *et al.* (1990). Use of wollastonite in the removal of Ni(II) from aqueous solutions. Water, Air, & Soil Pollution **49**(1): 69-79.

Sposito, G. (1986). On distinguishing adsorption from surface precipitation. In: Davis, J.A. and Hayes, K.F., (Editors). Geochemical Processes at Mineral Surfaces. ACS Symposium Series**.** Washington, DC, American Chemical Society. **323**: 217–228.

Sposito G. (1984). The Surface Chemistry of Soils. New York, Oxford University Press. 234 pp.

Stipp, S. L., Hochella M. F. Jr., *et al*. (1992). Cd^{2+} uptake by calcite, solid-state diffusion, and the formation of solid-solution: Interface processes observed with near-surface sensitive techniques (XPS, LEED, and AES). Geochimica et Cosmochimica Acta **56**(5): 1941-1954.

Stipp, S. L. S. (1999). Toward a conceptual model of the calcite surface: hydration, hydrolysis, and surface potential. Geochimica et Cosmochimica Acta **63**(19-20): 3121-3131.

Stumm, W. and Morgan, J.J. (1996). Aquatic Chemistry – chemical equilibria and rates in natural waters. 3rd edition. New York, Enviromental Science and Technology. 1005 pp.

Suthersan, S.S. (2001). Natural and Enhanced Remediation Systems. Florida, Lewis Publishers- Boca Raton. 440 pp.

Wang, Y. and Reardon, E. J. (2001). A siderite/limestone reactor to remove arsenic and cadmium from wastewaters. Applied Geochemistry **16**(9-10): 1241-1249.

Van Cappellen, P., Charlet, L. *et al.* (1993). A surface complexation model of the carbonate mineral-aqueous solution interface. Geochimica et Cosmochimica Acta **57**(15): 3505-3518.

Van der Weijden, R. D., Meima, J., *et al.* (1997). Sorption and sorption reversibility of cadmium on calcite in the presence of phosphate and sulfate. Marine Chemistry **57**(1-2): 119-132.

Villegas-Jimenez, A., Mucci, A., *et al.* (2009). Proton/calcium ion exchange behavior of calcite. Physical Chemistry Chemical Physics **11**(39): 8895-8912.

Zachara, J. M., Cowan, C. E., *et al.* (1991). Sorption of divalent metals on calcite. Geochimica et Cosmochimica Acta **55**(6): 1549-1562.

Chapter 2- Ni sorption behaviour on calcite: a macroscopic experimental study.

Lamana, T. and Mucci, A.

To be submitted to: Journal of Colloid and Interface Science

Abstract

Batch sorption experiments were conducted at ambient temperature (25±2ºC) and atmospheric pCO_2 ($10^{-3.41}$atm) in calcite pre-equlibrated NaCl solutions of distinct ionic strengths (0.1M to 0.7M) over a range of pH (7.5 to 8.9) and total nickel (Ni) concentrations (1.2 x 10^{-4} to 3.5 x 10^{-6} M). All solutions were under-saturated with respect to Ni-solid phases (e.g., gaspeite and nickel hydroxide). Results from kinetic experiments reveal that adsorption equilibrium was reached within the first 24 hours of reaction. Ni uptake by calcite in both ionic strength solutions was strongly pH dependent and correlated to the relative abundance of the $NiCO_3^0{}_{(aq)}$ species in solution. The adsorption data were modeled using Langmuir and Freundlich isotherms to quantitatively characterize the affinity of Ni(II) for the calcite surface. Irrespective of the solution ionic strength (0.1 and 0.7 M NaCl), the extent of Ni sorption reversibility was contingent upon the adsorbed Ni concentration.

2.1-Introduction

Calcite is the most thermodynamically stable calcium carbonate ($CaCO_3$) polymorph under earth surface conditions (Morse and Mackenzie, 1990). Due to its reactivity and ubiquity, it plays a major role in the chemistry of natural aqueous solutions

by regulating pH and alkalinity (Morse *et al*., 2007). Moreover, via sorption reactions, calcite may affect the mobility and geochemical cycling of trace metals (Van Cappellen *et al.* 1993, Villegas-Jimenez, 2009). Until now, a great deal of information has been gathered about the sorption properties of calcite, especially its propensity to sequester divalent cations such as Cd^{+2}, Pb^{+2} and Ni^{+2} (Davis et al. 1987; Zachara *et al.* 1991; Green-Pedersen *et al.* 1997; Lakstanov and Stipp, 2007).

Nickel (Ni) is an element of environmental concern; it is included in the US EPA "Red List" as a priority pollutant, and consequently a drinking water concentration threshold of approximately 52 ppb (8.85×10^{-7} M) is imposed in North America while 20 ppb (3.40×10^{-7} M) is the recommended limit by the World Health Organization (WHO). Nevertheless, the increasing demand for Ni-containing products (e.g. stainless steel) inevitably leads to increased discharge of Ni-rich wastewaters and atmospheric fallout derived from mines operations, smelters, refineries and the incineration of urban wastes, and its ultimate transfer to the biosphere (Denkhaus and Salnikow, 2002; Nieminen *et al.,* 2007). For this reason, many studies (e.g., Zachara *et al.,* 1991) have been carried out to develop new technological schemes for economic and safe Ni waste remediation and storage (Sharma *et al.*, 1990, Zachara *et al.,* 1991, Pedersen-Green *et al.*, 1997). In the industry, the use of natural minerals is becoming a popular choice in passive heavy metal-removal water treatment, due to its low maintenance cost, simple design and ease of operation (Sharma *et al.,* 1990). Optimally, these minerals should be readily available and inexpensive, and for this reason calcite has been regarded as a potential substrate for *in situ* metal scavenging (Rouff *et al.* 2002). Hence, a great deal of information has been gathered about sorption (a term commonly used to describe combined adsorption and co-

precipitation; Sposito, 1984; Zachara, 1991) properties of calcite, especially its propensity to sequester divalent metal ions such as Cd^{2+}, Zn^{2+} and Pb^{2+}.

The knowledge of factors that may control the fate of Ni in calcite-rich natural waters (e.g. groundwaters, carbonate-rich coastal and marine sediments) is critical, but there is scarce literature dedicated to the effect of mineral properties and solution composition on the affinity and sorption mechanisms between this metal and calcite. Hence, in order to provide new insights about factors that may promote or inhibit Ni(II) uptake by calcite, we investigated the influence of pH (7.5-9.5), ionic strength (0.1M and 0.7M), Ni(II) concentration and reaction times on the sorption of this metal on the calcite surface in NaCl solutions. Ni adsorption was described by isotherm models (Langmuir and Freundlich) in order to derive mass action relationships (K_{ads}). Finally, we provide novel information about the desorption behaviour of Ni(II) under our imposed experimental conditions. Ultimately, we expect that a better understanding of the mechanisms responsible for nickel uptake will improve modelling capabilities.

2.2-Material and Methods

2.2.1- Geochemical codes

The geochemical computer code PHREEQC (Parkhurst and Appelo, 1999) was used to simulate and predict the composition of the experimental aqueous solutions. According to the application manual, the speciation calculations return reliable results up to the ionic strength of seawater (0.7 M) upon implementation of the WATEQ4F thermodynamic database. LJUNGSKILE (version 2.0) is a probabilistic speciation code that was likewise coupled with the WATEQ4F database to construct speciation diagrams

(e.g. species abundance versus pH) with a confidence interval of 68% (Ödegaard-Jensen, *et al.* 2004; Merkel and Planer-Friedrich, 2008). All calculations were carried out for an open system at 25°C and a $pCO_2 = 10^{-3.41}$ atm.

2.2.2- Material preparation

All the laboratory glassware used throughout the experiments were acid-washed in a 10% HCl acid bath for a minimum of 24 hours, rinsed several times with Milli-Q® water and air-dried. Solutions were prepared in distilled water and all solid reagents (except $Ni(Cl)_2 \cdot 6H_2O$, 99.7% pure, Anachemia) were carefully oven-dried overnight on a watch-glass at 70ºC beforehand. Sodium chloride (NaCl; A.C.S grade reagent, ACP chemicals inc.) was used as the background electrolyte at different concentrations (0.1M and 0.7M). An initial Ni stock solution of 1000 ppm (~ 1.7×10^{-2} M) was prepared from nickelous II chloride, ($Ni(Cl)_2 \cdot 6H_2O$). This stock solution was then diluted in the background electrolyte to the desired Ni(II) initial concentrations for sorption kinetic and adsorption isotherm experiments.

2.2.2. a- Preparation of calcite pre-equilibrated solutions (CPES)

To minimize dissolution /precipitation of the reagent grade calcite substrate, but more importantly the co-precipitation of Ni on the calcite surface, the NaCl electrolyte solutions were previously equilibrated with calcium carbonate ($CaCO_3$) for up to two weeks at ambient temperature (±23ºC) and pressure ($pCO_2 = 10^{-3.41}$ atm) or until the pH stabilized at 8.29 ± 0.05. To maintain the electrolyte solutions calcite-saturated at all

times while varying pH, the solution total calcium concentration ($[Ca]_{total}$) or alkalinity ([Alk]) were increased by adding $CaCl_2$, $NaHCO_3$ or Na_2CO_3, respectively. The amount of $CaCl_2$, $NaHCO_3$ or Na_2CO_3 required to achieve different pH values was calculated using the geochemical computer code PHREEQC. Equilibrium was interpreted to be achieved when pH fluctuated by less than 0.05 pH unit throughout consecutive measurements over a week time period, and total Ca concentrations and alkalinity remained invariant. Prior to starting an experiment, the CPES were filtered on a 5.0 cm diameter Millipore® 0.45μm membrane filter.

2.2.2.b- Calcite substrate (reagent grade)

All batch experiments were carried out with Baker® "Instra-analysed flux" reagent grade calcite as the substrate. This calcite had been previously treated by the procedure described by Mucci (1986). Briefly, it was washed twice in Milli-Q water and size separated by settling through a 3-m long, 7.5-cm diameter Plexiglas core tube filled with Milli-Q water. The middle third portion of the settled $CaCO_3$ was freeze-dried. X-ray diffraction analysis of this $CaCO_3$ indicated that it was composed of at least 99% calcite.The particle size was between 3 and 7 μm, as determined by scanning electron microscopy. The specific surface area of 0.52 m^2/g was determined by the Kr-BET method.

2.2.3-Analytical methods

2.2.3.a- pH measurement

pH measurements were carried out at regular intervals throughout the equilibration period of the electrolyte solutions with $CaCO_3$ (CPES) and during all batch adsorption/desorption experiments using a combination glass-reference electrode (model GK2401C; Radiometer Analytical®). The electrode was calibrated on the N.B.S scale using three (4.01, 7.00, 10.00 at 25 ºC) NIST-traceable buffer solutions. Reproducibility of pH calibrations, carried out before and after measurements of a single solution, was better than 0.005 pH unit. Because of problems inherent to the use of glass electrodes calibrated using NIST buffers (i.e., infinite dilution convention) in strong electrolyte solutions, this measurement was only used to verify that steady-state conditions were maintained throughout batch experiments. Hence, the accuracy of the pH values measured here is estimated at ± 0.07 pH unit.

2.2.3.b-Alkalinity titration

Alkalinity of the experimental solutions was determined by potentiometric titration (TitraLab865® Titration Manager, Radiometer Analytical) with a dilute HCl solution (0.003N) of a known weight of the samples. Raw titration data were processed with a proprietary algorithm specifically designed for shallow end-point detection. Three solutions of different alkalinities were prepared gravimetrically using the alkalimetric

standard Na_2CO_3 salt and used for the standardization of the acid at the beginning and end of each day. The reproducibility of the measurements was better than 0.5%.

2.2.3.c-Atomic absorption spectrophotometry

Total Ni and Ca concentrations in each sample were determined using a Perkin Elmer AA-100 Atomic Absorption Spectrophotometer using an air-acetylene flame. The detection limits for the Ca and Ni analyses were 0.1 mg/L (2.5×10^{-6} M) and 0.02 mg/L (1.7×10^{-7}M), respectively. A minimum of five standard solutions (0.1-10mg/L) and a blank were prepared for each element. The blank was composed of either 0.1M or 0.7M NaCl plus 1% equivalent volume of metal grade HCl. Standards were prepared by appropriate dilution of 1000 ppm stock standard solutions (Plasmacal®, ICP-AES and ICP-MS standard, NIST traceable) in 4%HNO_3.

2.2.4-Batch experiments protocol

Batch sorption experiments were conducted under ambient temperature (25ºC ± 2 ºC) and atmospheric pCO_2 ($10^{-3.41}$atm) in calcite pre-equilibrated NaCl solutions of various ionic strengths (0.1M to 0.7M), nickel concentrations (1.2×10^{-4} to 3.5×10^{-6} M) and over a range of pH (7.5 to 8.9).

2.2.4.a- Kinetic uptake experiments

Time sequence experiments were carried out to identify the two major sorption processes (adsorption followed by co-precipitation, as schematically described by Davis

et al., 1987) of Ni uptake and to determine when steady state had been attained. One hundred (100) mL of a CPES were added to ten (10) 125-mL Erlenmeyer glass flasks. One (1) gram of reagent grade calcite was added to nine (9) of these solutions, for a final solid:solution ratio of 10 g/L, equivalent to a surface area:volume ratio of 5.2 m^2/L. This solid:solution ratio was the same in all batch experiments and similar (~5.0 m^2/ L) to the one adopted by Zachara *et al*. (1991). Blanks, comprised of calcite-free CPES solution served to determine the initial Ni concentration and its uptake by the walls of the reactor which, after 200 hours of contact, was negligible (<2.5%). Exactly 0.7 ml of the ~1.7 x 10^{-2} M $NiCl_2 \cdot 6H_2O$ concentrated stock solution was added to each flask. Each flask was gently hand-stirred once a day. Solutions from each batch were filtered through a Millipore® 0.45µm membrane filter (2.5-cm diameter) after approximately 1, 3, 6, 12, 24, 48, 72, 96 and 120 hours. Thirty (30) ml of each filtered solution were acidified with 1% v/v of concentrated metal grade HCl and served for the $[Ni]_{total}$ and $[Ca]_{total}$ analyses, while the remainder (70 ml) was analyzed for total alkalinity ([Alk]). Metals analysis took place within 24 hours after the end of experiments and all samples were stored in plastic (polypropylene) capped tubes at room temperature.

2.2.4.b-Adsorption Isotherms

The same procedure adopted for the kinetic experiments was reproduced here. One hundred (100) mL of a CPES were added to sixteen (16) 125 mL Erlenmeyer glass flasks. Adsorption experiments were carried out in only eight (8) of them and accordingly, the calcite substrate was added to these flasks. The remaining eight (8) flasks served to assess the $[Ni]_{total}$ initial concentration in each adsorption reactor. Disparities between

spiked volumes in the two flasks (adsorption reactor and blank) were confirmed to be negligible (<0.1%). The $[Ni]_{total}$ initial concentration ranged from $1.2x10^{-4}$ - $3.5x10^{-6}$ M. For this experiment, reactions with the calcite were allowed to proceed for approximately 24 hours.

2.2.4.c- Desorption experiments

Following the Ni(II) adsorption experiments, desorption was initiated by replacing the supernatant solution with an equivalent volume of a Ni-free CPES to each flask. The membrane filter holding the calcite powder recovered from the previous adsorption experiments was immersed into 50 mL of Ni-free CPES in an Erlenmeyer, and the extra 50 mL of the Ni-free CPES were used to rinse the glass filtration funnel to ensure a quantitative recovery of the calcite particles used in the previous adsorption experiments. The re-suspended Ni-reacted calcite particles were equilibrated with the Ni-free CPES for twice as long as it spent in the adsorption reactor (i.e., ~48 hours).

2.3- Results

2.3.1- Aqueous speciation

According to calculations performed with PHREEQC and the speciation diagrams generated by LJUNGSKILE 2.0 (Figs. 2.1 and 2.2). In the 0.1 M NaCl CPES, $Ni^{2+}_{(aq)}$ is the most abundant species below pH 7.7; its maximum relative abundance (82%) was registered at pH 7.1. Between pH 7.7 and 8.7, $NiCO_3^0{}_{(aq)}$ predominates (maximum of 90% at pH 8.3) whereas $Ni(CO_3)_2^{-2}{}_{(aq)}$ becomes the dominant species above pH 8.7. In 0.7 M NaCl CPES, there is a decrease in the relative abundance of the $NiCO_3^0{}_{(aq)}$ complex (from 90% to 85% at pH 8.3) as well as Ni^{+2} (from 71% to 42% at pH 7.3), coupled with an

increase in total chloride species, in particular $NiCl_{2(aq)}$ (Fig. 2.2). Over the pH range at which the experiments were carried out, $NiCl_2$, $NiOH^+$ and $Ni(OH)_2$ accounted for less than 1% of the total Ni (II) species in both solutions (0.1 and 0.7 M NaCl) and their representation was excluded from the speciation diagrams.

2.3.2- Equilibrium calculation

Simulations were run in PHREEQC to predict the maximum $[Ni]_{total}$ concentration that could be added to CPES as a function of pH before reaching saturation with respect to $Ni(OH)_{2(s)}$ and $Ni(CO)_{3(s)}$. The mineral solubility products (K_{sp}) were taken from the WATEQ4F database ($10^{-10.80}$ and $10^{-6.84}$ for $Ni(OH)_{2(s)}$ and $Ni(CO)_{3(s)}$ respectively), though reported values for $Ni(OH)_{2(s)}$ in the literature vary by up to seven orders of magnitude (from $10^{-19.02}$ to 10^{-11}) (Mattigod *et al.,* 1997). This discrepancy has been attributed to the variability of the $Ni(OH)_{2(S)}$ crystallinity (ranging from "freshly" precipitated: log K^0_{sp} = -15.2, to an aged solid: log K^0_{sp} = -16.9 to -17.5) (Villegas-Jimenez *et al.,* 2010). Hence, we decided to maintain the value reported in the WATEQ4F database (Ball and Nordstrom, 1991). For all simulations, the solutions reached $Ni(OH)_{2(s)}$ saturation, before reaching saturation with respect to $Ni(CO)_{3(s)}$. Hence, based on the conditions under which we carried out our experiments, calculations revealed that the maximum $[Ni]_{total}$ concentration present in the aqueous phase could range from 1.5 x 10^{-4} M (pH 7.5) to 2.9 x 10^{-4} M (pH 8.3) in the 0.1M NaCl solution and from 1.2 x 10^{-4} M (pH 7.5) to 4.2 x 10^{-4} M (pH 8.3) in the 0.7 NaCl solution (Fig. 2.3). Additionally, as expected for a calcite saturated solution at a fixed pCO_2 ($10^{-3.41}$ atm), the $[Ca]_{total}$ concentration decreased as $[Alk]_{total}$ concentration increased with pH.

2.3.3-Sorption kinetics

With one exception (0.1 M NaCl solution at pH 7. 82), Ni uptake increased with time and pH (Fig. 2.4). For the 0.1 M NaCl solution at pH 7.82, a very rapid increase (from 0 to 7%, Fig. 2.4.A) of Ni sorption took place during the first hour of reaction, after which it decreased (from 7% to 2%) until it reached equilibrium after approximately 24 hours (Fig. 2.4.A). A similar behaviour was observed in the 0.7 M NaCl solution at pH 7.68, but a transient state was apparently achieved after about 12 hours of contact between Ni(II) and calcite before Ni uptake proceeded at a slow rate (Fig. 2.4.A). In 0.7M NaCl at pH 8.06 and 0.1M NaCl at pH 8.26 (Figs. 2.4.B and C), sorption appeared to achieve equilibrium between 10 and 50 hours. Conversely, clear evidence of equilibrium was only observed in 0.1M NaCl at pH 8.02 (Fig. 2.4.B) and 0.7 M NaCl at pH 8.32 (Fig. 2.4.C) and 8.68 (Fig. 2.4.D), where the fractional sorption remained constant after approximately 24 hours. In 0.1 M NaCl solution at pH 8.65, Ni sorption was slower and proceeded further after 24 hours of reaction. The designated two step sorption process, a fast uptake followed by either equilibrium or slower uptake rate, was not observed in the 0.1 M NaCl solution at pH 8.84 and in 0.7 M NaCl at pH 8.95 as fractional sorption increased dramatically after 50 hours of reaction, reaching nearly 100% (Fig.2.4.E).

2.3.4-Adsorption edge

Since Ni sorption exhibited mainly two different types of behaviour with reaction time (i.e., initial fast uptake within the first 24 hours, followed by either equilibrium or a progressive uptake), we compiled the data obtained within the first 24 hours of reaction, presumably reflecting mostly adsorption, in order to compare results obtained at the two

ionic strengths. Within this time interval, there was a general increase in Ni adsorption with increasing solution pH (Fig. 2.5). Below pH 8.06, fractional sorption was less than 10% in both 0.1M and 0.7 M NaCl solutions. The Ni adsorption edge (a sharp increase of adsorption within a narrow range of pH) in 0.1 M NaCl was observed within the 8.06-8.65 pH range whereas, in 0.7M NaCl, fractional adsorption nearly doubled between 8.32 and 8.68. Beyond pH 8.65, adsorption decreased from approximately 40% to 25% in the 0.1M NaCl solution, but increased slightly beyond pH 8.68 (from 34% to 36%) in the 0.7M NaCl solution.

2.3.5-Adsorption isotherm

No adsorption experiment was carried at 0.1M NaCl below pH 8.02, because kinetic experiments revealed that, under these conditions, the fractional Ni uptake did not exceed 8% when the $[Ni]_{total}$ was approximately 1.0×10^{-4} M. Hence, at the lower initial $[Ni]_{total}$ concentrations, changes in the bulk $[Ni]_{total}$ would not be detected. For instance, disparities between $\Gamma[Ni]_{ad}$ (adsorbed Ni concentration per m^2 of calcite) results obtained in 0.1M and 0.7M NaCl (for solutions with a fixed pH value) were considered minor, when the $[Ni]_{eq}$ (total Ni concentration present in the system by the end of the experiment) was below 1.0×10^{-5} M. In all systems investigated, regardless of solution pH or ionic strength, $\Gamma[Ni]_{ad}$ increased with increasing $[Ni]_{eq}$ (Fig.2.6). Notably, the adsorption isotherm data in both 0.1M and 0.7 M NaCl solutions exhibited the same trend previously described at the adsorption edge (Fig. 2.7).

In order to identify the binding capacity of the calcite surface, two adsorption models were applied. The Langmuir model assumes that adsorption occurs at all surface

sites, that these are identical (same energy) and non-interacting and equilibrium is reached upon the formation of a monolayer of adsorbates (implying the saturation of adsorption sites). The Freundlich model typically applies to solids with heterogeneous surface properties where saturation of the adsorption sites does not occur and multilayer adsorption of adsorbates is possible (Stumm and Morgan, 1996). Under equilibrium conditions, and considering that all the major chemical variables (e.g., pH and ionic strength) are constant, a simple mass action law (Eqn.1) should apply to describe Ni adsorption within our systems, according to:

$$\mathbf{>S + Ni(II)_{(eq)} \leftrightarrow >SNi} \qquad (1)$$

$$\mathbf{K_{ads} = [\ >SNi]/\ [>S]\bullet[Ni(II)_{(eq))}]} \qquad (2)$$

where **>S** represents calcite surface sites, $\mathbf{Ni(II)_{(eq)}}$ is the total Ni concentration in solution at equilibrium, **>SNi** is the Ni bonded to the surface site. If the Langmuir model is applied, $\mathbf{\Gamma[Ni]_{ad}}$ = **[>SNi]**/calcite surface area, $\mathbf{\Gamma_{max}}$ = **([>S] + [>SA])**/calcite surface area and $\mathbf{K_{ads}}$ may be derived from Eqn. 2 as:

$$\mathbf{\Gamma[Ni]ad = \Gamma_{max} \bullet Kads \bullet [Ni(II)_{(eq))}] \,/\, 1 + (K_{ads} \bullet [Ni(II)_{(eq))}])} \qquad (3)$$

where $\mathbf{\Gamma[Ni]_{ad}}$ is the Ni adsorption density and $\mathbf{\Gamma_{max}}$ is the maximum adsorption capacity of the system. The K_{ads} and $\mathbf{\Gamma}_{max}$ were readily obtained from the linear regression of the experimental data when plotted as the reciprocal of Eqn. 3 (Table 2.1).

The Freundlich equation is often written as:

$$\mathbf{\Gamma[Ni]_{ad} = \mathit{m}[Ni(II)_{(eq))}]^n} \qquad (4)$$

where *m* is referred to as the Freundlich reaction constant and n is a measure of the non-linearity of the adsorption process. When n is greater than 1, the extent of adsorption increases with increasing metal concentration (not necessarily this increase is

proportional). Conversely, if n is lower than 1, the adsorption data will display decreased relative adsorption with increasing metal concentration. For convenience, the Freundlich isotherm was plotted in double logarithmic form and, thus, expressed as:

$$\mathbf{log\Gamma[Ni]_{ad} = log}\boldsymbol{m} \mathbf{+ nlog[Ni(II)_{(eq)})]} \quad (5)$$

In 0.1M NaCl, Langmuir K_{ads} decreased by (from $10^{6.34}$ to $10^{1.76}$) with increasing solution pH, while Γ_{max} increased by about one order of magnitude from pH 7.98 to pH 8.26 and decreased thereafter (Table. 2.1). When the Freundlich model was applied to the same data set, *m* increased systematically with solution pH, coupled with increasing n (from 0.69 to 1.01). Above pH 8.26, both *m* and n decreased with increasing pH. In 0.7M NaCl, beyond pH 8.26, K_{ads} also decreased ($10^{7.01}$ to $10^{1.51}$) with increasing solution pH while Γ_{max} remained nearly constant ($\pm 3.83 \times 10^{-6}$ mol/m^2). Notably, at the same ionic strength, the Freundlich model coefficients exhibit a clear trend with *m* and n increasing with solution pH (Fig. 2.9).

2.3.6-Desorption

Desorption was determined by comparing the ratios of Ni adsorption density after ($\Gamma[Ni]_{ad'}$) and prior ($\Gamma[Ni]_{ad}$) to the desorption experiments. Desorption was considered to be complete if $\Gamma[Ni]_{ad'}$ and, hence, the $\Gamma[Ni]_{ad'}$:$\Gamma[Ni]_{ad}$ ratio was equal to zero, indicating that all Ni desorbed from the calcite surface. A complete desorption was not expected, instead a new equilibrium would be established. If the $\Gamma[Ni]_{ad'}$ and $\Gamma[Ni]_{ad}$ have the same value ($\Gamma[Ni]_{ad'}/\Gamma[Ni]_{ad} = 1$), then no Ni was detected in solution and the reaction was considered to be irreversible. Accordingly, the greater the ratio deviates from 1, the greater the tendency of Ni to desorb from the calcite surface. It was observed that, in 0.7

M NaCl between pH 7.59 and 8.06, Ni desorption decreased with increasing $[Ni]_{eq}$ concentration (Fig. 2.9). In the same electrolyte solution (0.7M NaCl), at pH 8.32 and above a $10^{-4.4}$M $[Ni]_{eq}$ concentration, desorption was analogous to the profile displayed in solution with lower pH values (7.59 and 8.06). The same trend was observed at higher Ni ($10^{-4.8}$M to $10^{-4.4}$M) concentrations at pH 8.66, but the data below this concentration range were ambiguous. At pH 8.63 in 0.1M NaCl solution, no evidence of desorption was detected. Similarity, at pH 8.26 above $10^{-4.4}$ M of $[Ni]_{eq}$, the desorption ratios were approximately one (> 0.92). At pH = 7.98, desorption decreased with increasing $[Ni]_{eq}$ ($\Gamma[Ni]_{ad'}/\Gamma[Ni]_{ad}$ = 0.59 to 0.97). Surprisingly, in 0.7M NaCl at pH 8.95, desorption increased with increasing total $[Ni]_{eq}$, whereas, in 0.1M NaCl at pH 8.9, Ni desorption decreased with increasing $[Ni]_{eq}$.

2.4-Discussion

2.4.1-The solubility of $Ni(OH)_{2(s)}$

Nickel forms a relatively insoluble hydroxide, $Ni(OH)_{2(s)}$, in alkaline solutions, and its solubility can be used to set upper limits on the $[Ni]_{total}$ concentration in those systems. In calcareous aqueous systems, nickel carbonate ($NiCO_{3(s)}$) should likewise be taken into account in determining the limits imposed by its solubility on the total Ni present in the aqueous phase. As $NiCO_{3(s)}$ precipitation never occurs alone but in competition with nickel hydroxide ($Ni(OH)_{2(s)}$) (Guillard and Lewis, 2001), the calculations carried out with PHREEQC revealed that, under the conditions imposed in this study, the precipitation of a Ni solid phase is mainly dictated by $Ni(OH)_{2(s)}$ solubility. Nevertheless, the precipitation of a mixed nickel hydroxy-carbonate, whose composition is expected to depend on the carbonate (CO_3^{-2}) to Ni ratio within the system, is possible.

The $[CO_3^{-2}]$:$[Ni]_{total}$ ratio varies with solution pH and reaches its maximum at approximately pH 8.3. As shown on Fig. 2.3, the initial $[Ni]_{total}$ that was added at the onset of kinetic experiments is below the $Ni(OH)_{2(s)}$ saturation domain. All $[Ni]_{total}$ used in the isotherm experiments were below the initial concentrations of the kinetic experiments at any given pH value. Hence, it is reasonable to assume that a decrease in $[Ni]_{total}$ during the kinetic and adsorption experiments were not caused by a distinct Ni solid precipitation.

2.4.2- Ni sorption rate

The rates of divalent metal sorption by calcite have usually been characterized by an initial fast uptake followed by a slower fractional sorption, with half-times of reaction occurring on the order of minutes (fast) and hours to days (slow). Previous researchers have ascribed that the fast process to adsorption of those metals onto the surface, and the slower process to co-precipitation through re-crystallisation or even entrapment into defect sites (Davis *et al.*, 1987; Rouff *et al*., 2002; Lakshtanov and Stipp, 2007). Since re-crystallisation is driven by the difference in surface free energy for crystals of different sizes and that metastable solid phases can be formed (Zachara *et al*., 1991), the likelihood of co-precipitation of an adsorbed Ni(II) into freshly formed calcite surface layers is considerable (Lakshtanov and Stipp, 2007). Although ageing of the calcite substrate, prior to experimental use, should have reduced the number of defect sites. Nonetheless, the adsorption of Ni on calcite surface active sites decreases the mineral's solubility and likewise induces the re-crystallization (Green-Pedersen *et al.*1997). As described by Davis *et al.* (1987) with respect to cadmium (Cd(II)), the first 24 hours of reaction was

critical for the Ni(II) reaction with the calcite surface and, based on the results of our experiments, adsorption equilibrium was estimated to be reached within 24 hours. Hence, in the present study, adsorption and co-precipitation were distinguished based on the sorption kinetic (as well as desorption behaviour), but we acknowledge the potential weakness of this approach because it did not involve a direct microscopic characterization of the calcite surface. Nevertheless, this study is novel since, to our knowledge, the Ni sorption behaviour on calcite in NaCl solutions of various ionic strengths has never been investigated. Based on the results of this macroscopic study, we identify the main chemical variables that control Ni(II) sorption in similar natural systems, such as carbonate aquifers and carbonate-rich coastal and marine sediments.

2.4.3- The influence of chloride (Cl) on Ni sorption

The main difference between our and previous studies (Zachara *et. al.,*1991; Hoffman and Stipp. 2001; Lakshtanov and Stipp. 2007; Belova *et al.* 2008) of Ni(II) sorption on calcite is the replacement of sodium perchlorate ($NaClO_4$) by NaCl as a background electrolyte. Despite its strongly oxidizing nature, ClO_4^- is stable and forms weak complexes with metal ions in aqueous solutions because of its high ionic size (i.e. 2.4Å) and low charge density (Brown and Gu, 2006). It also binds weakly to solid surfaces (i.e. poor coordinating ability). In Zachara *et al.* (1991), the maximum Ni sorption registered under their experimental conditions (25°C, $pCO_2 = 10^{-3.5}$ atm, total metal concentration on the order of 10^{-7} mol L^{-1}, approximately 5.0 m^2 L^{-1} of calcite particle loading and 24 hours of reaction in 0.1M $NaClO_4$ calcite-saturated solution) was approximately 60% at ~pH 9.2 and the adsorption edge was constrained between pH 8.0

and 9.0. Belova *et al.* (2008) carried out experiments under very similar conditions, at an initial metal concentration of ~10^{-5} M and surface area:volume ratio of 17.25 m^2 L^{-1}, and reported a maximum of 65% Ni sorption at pH 8.7 and an adsorption edge ranging from 8.1 to 8.8. Under our experimental conditions, we observed a maximum of 40 % Ni sorption in 0.1M NaCl at pH 8.65 and 36% in 0.7M NaCl at pH 8.9 whereas the adsorption edges in both 0.1M NaCl (pH 8.06 to 8.65) and 0.7M NaCl (pH 8.32 to 8.68) were considerably narrower than those observed by Zachara *et al.* (1991) and Belova *et al.* (2008). A possible interpretation of the differentbehaviour is that the presence of a ligand (i.e. Cl^-) in solution would decrease the overall sorption of Ni on the calcite surface (Fig. 2.5).

2.4.4- The role of the $NiCO_3^0{}_{(aq)}$ complex

Although it has not yet been emphasized by other researchers, the relative abundance of the $NiCO_3^0{}_{(aq)}$ species appears to greatly influence the overall Ni adsorption behaviour on the calcite surface (Fig. 2.5). Following the same principle adopted by Rouff *et al.* (2005) in their study of Pb(II) sorption, we propose that the presence of the neutral species $NiCO_3^0{}_{(aq)}$ may facilitate the interaction of Ni(II) with the calcite surface regardless of the mineral's net surface charge at a given solution pH. Accordingly, the fractional Ni(II) adsorption correlates well with the relative abundance of $NiCO_3^0{}_{(aq)}$ at all pH values. The decrease in Ni(II) sorption above pH 8.65 in 0.1 M NaCl is possibly linked with the attenuation of $NiCO_3^0{}_{(aq)}$ abundance in this system. Despite of the apparent difference in the pH range over which $NiCO_3^0{}_{(aq)}$ is the dominant Ni(II) species (7.7 to 9.1 rather than 7.7 to 8.9 in 0.1 M NaCl) in the 0.7 M NaCl solution a t-test

revealed that there is no significant difference (*p*-value = 0.31) between the relative abundance of $NiCO_3^0{}_{(aq)}$ in the two electrolyte systems.

2.4.5- Adsorption isotherms

The {1014} calcite plane is the most commonly observed on commercially available calcite due to its stability and preferred cleavage. Its unit cell lattice surface is described as being 4.99Å wide and 8.10Å long and comprises two Ca and two CO_3 groups per 40.42Å^2 (Reeder, 1983; Lakshstanov and Stipp, 2007). Thus, the theoretical calcite lattice site density, estimated from the atomic spacing, is about 5 x 10^{-18} sites m^{-2} or 8.22 x 10^{-6} mol of sites per m^2 of calcite surface, for cations or anions (Lakshstanov and Stipp, 2007). Nonetheless, all Γ_{max} values derived from our Langmuir model fits, irrespective of the electrolyte system, are greater than the theoretical calcite site density (Table 2.1). A similar observation was reported by McBride (1979) in his study with Mn(II) (25°C; atmospheric $pCO_{2(g)}$; $[Mn]_{total}$ ranging from 10^{-3} to 10^{-6}M). It was suggested that at low $[Mn]_{eq}$ (<10^{-5}M), the metal binds to the surface via chemical bonding, and, as $[Mn]_{eq}$ increases, Mn(II) would co-precipitate or even form a surface precipitate (subsequent nucleation and precipitation of $MnCO_3$ on the calcite surface) which notably surpasses the uptake capacity predicted for the formation of a single adsorbate monolayer.

Furthermore, in this study, the empirical coefficients (*m* and n) derived from the Freundlich model fits were consistent with the increased Ni(II) affinity for the calcite surface with increasing solution pH in 0.7 M NaCl solutions (Fig. 2.7). Moreover, in the same solution, it was noted that the n value increased sharply (2-3 fold) above pH 8.26,

which is reflected by the exponential increase in $\Gamma[Ni]_{ad}$. Sposito (1986) proposed that when adsorption isotherms arch upwards at higher adsorbate concentrations, adsorption alone may not control the uptake process, and co-precipitation may dominate under these conditions. This interpretation is a suitable interpretation of the results obtained in 0.7 M NaCl between pH 8.66 and 8.95 (Fig. 2.7). Based on our modelled adsorption data, we believe that in both the 0.1 M and 0.7 M NaCl solutions, the Freundlich model provides a more coherent representation of the interaction(s) between Ni(II) and the calcite surface, as revealed by our kinetic and adsorption isotherm data. It is important to note that the absolute value of the mass action constants (K_{ads} and *m*) derived from adsorption isotherm models are strictly conditional and can only be applied under the experimental conditions of this study. Nevertheless, the magnitude of these values provides insights on the affinity of Ni for the calcite surface (Green-Pedersen *et al.*1997).

2.4.6- Desorption

Desorption reactions were allowed to proceed for twice (approximately 50 hours) as long as the calcite had spent in contact with the Ni-bearing solution. This approach was based on previously reported observations that desorption rates of metal ions from the calcite surface are significantly lower than their adsorption rates despite being dynamic processes (Davis *et al.* 1987; Zachara *et al.* 1991; Rouff *et al.* 2002). If Ni(II) interacts electrostatically with the calcite surface, its propensity to undergo desorption would be greater than if the interaction is chemical (it forms chemical bonds with calcite surface groups). It was observed that desorption generally decreased with increased $[Ni]_{eq}$ (above 2.5×10^{-5} M at pH 8.66, and above 4.0×10^{-5} M in all our experimental solutions, with the

exception of 0.7M NaCl at pH 8.95) which may suggest that the interaction of Ni(II) with the calcite surface is mostly chemical.

2.4.7- Possible mechanisms of Ni uptake

Consideration should be given to the potential effects of calcite surface speciation and charge on the Ni adsorption mechanisms. According to solution pH as well as the hydration and adsorption of constituent ions from solution on the calcite surface, the following surface species: $>CO_3^-$, $>CO_3Ca^+$, $>CaO^-$, $>CaOH_2^+$, $>CaHCO_3^0$ and $>CaCO_3^-$, may form (Pokrovsky *et al.* 2000). This explains the amphoteric (acid-base) behaviour of the calcite surface, as protonated carbonate surface groups ($>CO_3H^0$) dominate in acidic solutions and hydrated calcium groups ($>CaOH_2^+$) are more abundant in neutral-alkaline solutions (Pokrovsky and Schott, 2002). It has been proposed that changes in calcite surface speciation with pH may result in subtle differences in sorbed metal configuration, influencing metal susceptibility to co-precipitation (Wolthers *et al*. 2004).

Nevertheless, the calcite surface electrical charge develops not only because of its amphoteric behaviour, but also in response to the adsorption of "potential determining ions ($PDI_{(s)}$)", such as constituent (Ca^{2+}, CO_3^{2-}) and other ions (e.g. HCO_3^-, Ni^{2+}) on the mineral surface. A net positive or net negative surface charge induces the migration of oppositely-charged ions in solution towards the surface to compensate for local surface imbalances (Moulin and Roques, 2003). For instance, the points of zero charge on a mineral's surface are pH values (pH_{pzc}) where the net surface charge is zero (Stumm and Morgan, 1996). Considering solely the adsorption/desorption of H^+ and OH^-, calcite surface neutrality would occur at pH_{pznpc} (pH of zero net proton charge when $\Gamma_{H^+} = \Gamma_{OH^-}$).

Mishra (1976) estimated the calcite pH_{iep} (isoeletric point pH, where no electrophoretic mobility occurs at the mineral surface) to be equal to 8.2, under the assumption that the specific adsorption of other ions (e.g. Ca^{2+}, CO_3^{2-}, HCO_3^-) in solution is minor $pH_{iep} \approx pH_{pnzpc}$ (Stumm and Morgan, 1996). Hence, it is reasonable to imply that above pH 8.2 (though a wide range of values is reported in the literature, because other PDIs contribute to the surface charge), the net calcite surface charge is negative. However, the only Ni(II) cationic species present in solution above pH 8.2 is Ni^{2+} (more likely present as $Ni \cdot 6H_2O^{2+}$; Neilson and Enderby, 1978), whose relative abundance in 0.1M NaCl and 0.7M NaCl does not exceed 6% of the $[Ni]_{total}$, thus, the electrostatic attraction of cationic Ni(II) species to the calcite surface is most likely minor.

McBride (1997) refined a pre-existing concept (Stumm and Morgan, 1996) about the ionic strength dependence of adsorption as an indirect method to distinguish between inner (chemical interaction) and outer-sphere (long-range interaction) surface complexation. He stated that decreased adsorption with increasing ionic strength reveals that ions are more likely to adsorb as an outer-sphere complex, whereas invariant adsorption behaviour with increasing ionic strength indicates the formation of an inner-sphere adsorption complex. Our adsorption isotherms (Fig. 2.6) revealed that, at lower pH values (pH 7.98 and 8.26), Ni(II) adsorption proceeds independently of the NaCl concentration, which may suggest that, under these conditions, Ni(II) adsorbs as an inner-sphere complex onto the calcite surface. Nevertheless, discrepancies were observed at higher pH values (between 8.66 and 8.95) in solutions containing $[Ni]_{eq}$ above 1.0×10^{-5}M. We observed that the extent of Ni desorption was contingent upon $[Ni]_{eq}$ of the system and that, at higher $[Ni]_{eq}$ ($> 4.0 \times 10^{-5}$M), adsorption most likely occurs through chemical bonding.

Kinetics of attachment of molecules to a growing solid-phase during re-crystallization have been shown to be related the activation energy of co-precipitation, which can be contingent upon the need to expel waters attached to the adsorbing ions (Petsev *et al.* 2003; Kowacz *et al.* 2010). This may explain the difficulty of pure $NiCO_3$ (gaspeite) to form at room temperature, whereas the compounds $NiCO_3{\cdot}2Ni(OH)_2$ or $NiCO_3{\cdot}4H_2O$ (zaratite) readily precipitate from aqueous solutions, suggesting that the dehydration of solvated Ni^{2+} ions requires much energy (Hoffman and Stipp, 2001). Likewise, the co-precipitation of Ni^{2+} with calcite is expected to be slower than for Cd^{2+} and Zn^{2+}, because they are larger ions and consequently their hydration energies are lower (-1801.42 kJ·mol$^-$ and -2027.80 kJ·mol$^-$ respectively; Hoffman and Stipp, 2001). Zachara *et al.* (1991) had already correlated the ionic radius size of divalent metals with their hydration energy (inverse variation with the ionic radius size) to infer that Ni^{2+}, as well as Zn^{2+} and Co^{2+}, would form surface complexes on calcite and these would remain hydrated until their incorporation into the bulk structure by re-crystallization. This hypothesis was later reiterated by Hoffman and Stipp (2001), based on results of their study (open system in equilibrium with atmospheric pCO_2, but undersaturated with respect to calcite and Ni solid phases) of the mechanisms of Ni incorporation in calcite, using surface sensitive techniques (XPS, TOF-SIMS and AFM). They showed that Ni^{2+} is accommodated into the calcite structure by surface relaxation (at pH 4.6).

In their study of barite ($BaSO_4$) precipitation at 25°C in a closed cell reactor, Kowacz and co-works (2010) reported that the increase in NaCl concentration decreased the water exchange rate around the crystal building units and consequently increased nucleation rates. Inspired by this hypothesis, we propose that Ni(II) most likely co-precipitates into calcite in 0.7M NaCl systems. Since $NiCO_3^0{}_{(aq)}$ is weakly hydrated (due

to its neutrality), the loss of its hydration shell and subsequent diffusion into the bulk solid should be facilitated in 0.7M NaCl relative to the lower ionic strength (0.1M NaCl) solutions. This may explain the observed in adsorption isotherm data above pH 8.66, as Ni(II) adsorption density increased exponentially with increasing $[Ni]_{eq}$, most likely reflecting co-precipitation.

Goldberg and co-workers (2007) provided an extensive list of potential sorption mechanisms (identified by spectroscopic methods) of divalent metal ions. They cite ten different investigations of Ni interaction with different minerals (e.g. gibbsite, kaolinite, montmorillonite, talc, silica, manganese hydroxide and pyrophillite) and the principal form of interaction of Ni(II) with these surfaces was through chemical bonding. Likewise, our findings, along with those of Hoffman and Stipp (2001) and Lakshtanov and Stipp (2007), emphasize that Ni(II) interaction with calcite occurs via chemical bonding with subsequent co-precipitation into the bulk solid.

2.5- Summary and conclusions

In this study, we investigated the influence of solution chemistry on the interaction between dissolved Ni(II) and the calcite surface. Our results highlight the effects of time, pH, ionic strength and $[Ni]_{total}$ in open calcite pre-equilibrated aqueous solutions. Uptake kinetic experiments revealed that the first 24 hours of reaction (interpreted as adsorption) were crucial for the uptake of Ni(II) by calcite, after which reaction either reached equilibrium (plateau) or progressed more slowly (reflecting metal co-precipitation). Like other divalent metal ions, Ni(II) sorption on calcite was strongly dependent on solution

pH. A detailed speciation analysis reveals that the pH-dependence is correlated to the relative abundance of the $NiCO_3^0{}_{(aq)}$ species in solution. The fractional sorption of Ni(II) was attenuated beyond pH 8.66 in 0.1M NaCl solution as the relative abundance of $NiCO_3^0{}_{(aq)}$ decreased. In contrast, in 0.7 M NaCl, fractional Ni sorption continued to increase beyond pH 8.66 because the field of stability of $NiCO_3^0{}_{(aq)}$ is shifted to higher pHs in this solution. The affinity of this complex for the calcite surface may be due to its ease of dehydration.

The adsorption isotherm results revealed that a Freundlich model provided a more coherent representation of the interaction between dissolved Ni and the calcite surface. In 0.7M NaCl solutions, the adsorption coefficients of non linearity (n) were all above the value of one (1). Our interpretation of this observation is that co-precipitation is the likely mechanism by which Ni(II) interacts with the mineral surface. Additionally, as $NiCO_3^0{}_{(aq)}$ is weakly hydrated (due to its neutrality), it may lose its hydration and co-precipitate into calcite bulk solid, to a greater extent in the 0.7M NaCl than in the 0.1M NaCl solution. Moreover, irrespective of the ionic strength (0.1M or 0.7M NaCl), the desorption of Ni(II) at higher $[Ni]_{eq}$ ($> 4.0 \times 10^{-5}$M) was limited, emphasizing our previous hypothesis that the interaction of Ni(II) with the calcite surface is most likely chemical. Finally, in comparison to the affinity of divalent metal cations such as Cd^{2+}, Pb^{2+} and Zn^{2+}, the extent of Ni sorption on calcite is moderate.

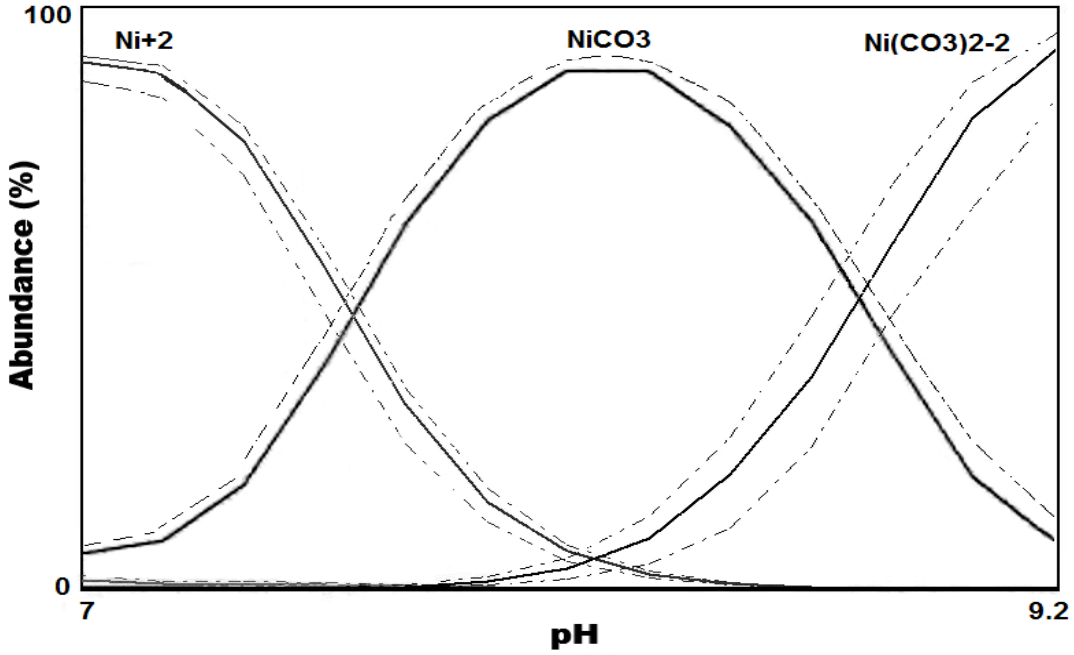

Figure 2.1- Ni(II) speciation as a function of pH at 10^{-4} M total Ni concentration, pCO_2 = $10^{-3.41}$ atm, 25°C in a 0.1 M NaCl calcite-equilibrated solution. This diagram was built using the LJUNGSKILE 2.0 application. Solid lines represent the mean from which the confidence interval of 68% range was derived (dashed lines).

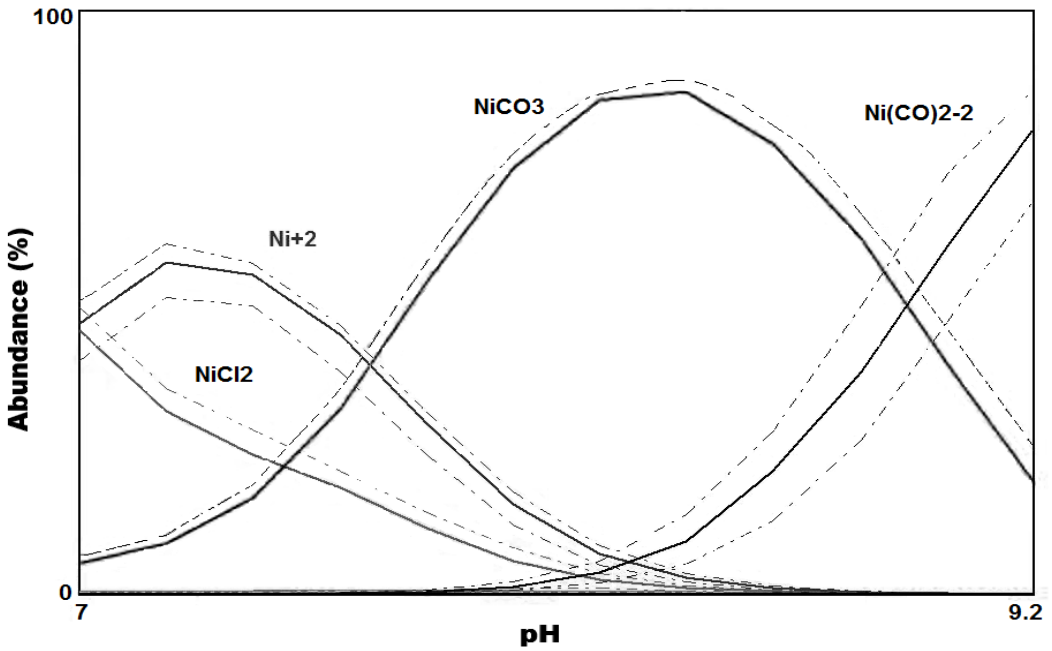

Figure 2.2- Ni(II) speciation as a function of pH at 10^{-4} M total Ni concentration, pCO_2 = $10^{-3.41}$ atm, 25°C in a 0.7 M NaCl calcite-equilibrated solution. This diagram was built using the LJUNGSKILE 2.0 application. Solid lines represent the mean from which the confidence interval of 68% range was derived (dashed lines).

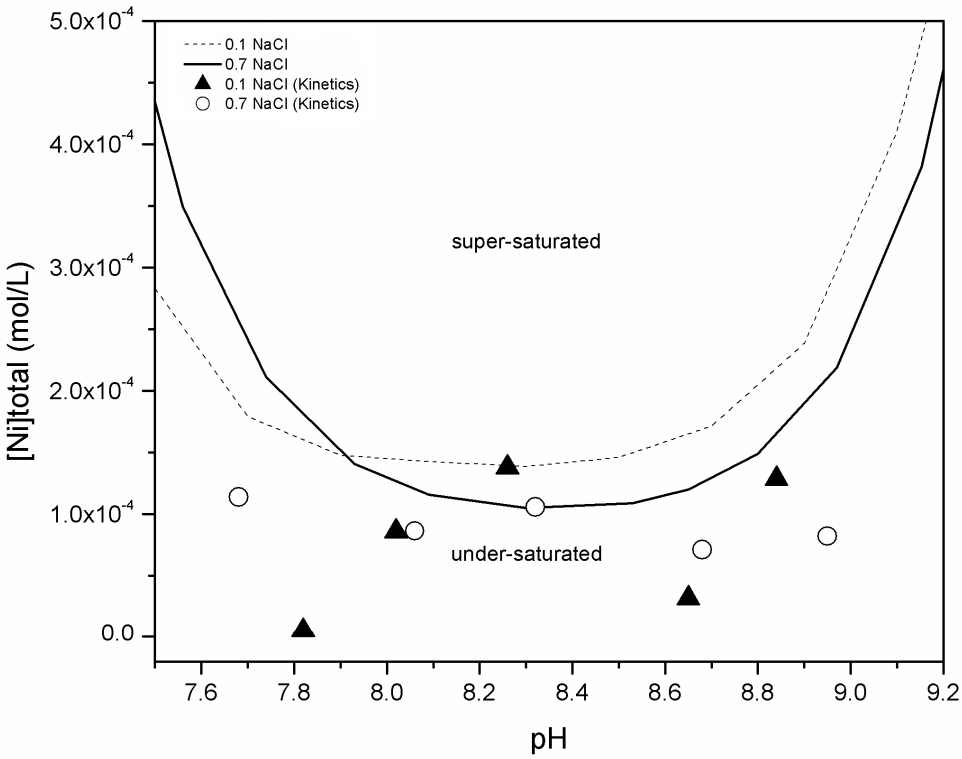

Figure 2.3- According to equilibrium calculations performed on PHREEQC, the dashed (---) and the solid (—) lines represent, respectively, the solubility of $Ni(OH)_{2(s)}$ in a solution in equilibrium with calcite at a $pCO_2 = 10^{-3.41}$ and 25°C when the background electrolyte is comprised of a 0.1 M or 0.7 M NaCl solution. The triangles (▲) and circles (○), represent the total Ni(II) concentration ($[Ni]_{total}$) added, respectively, to a 0.1 M and 0.7 M NaCl solution at the onset of kinetic experiments carried out in calcite-equilibrated solutions of different pH values.

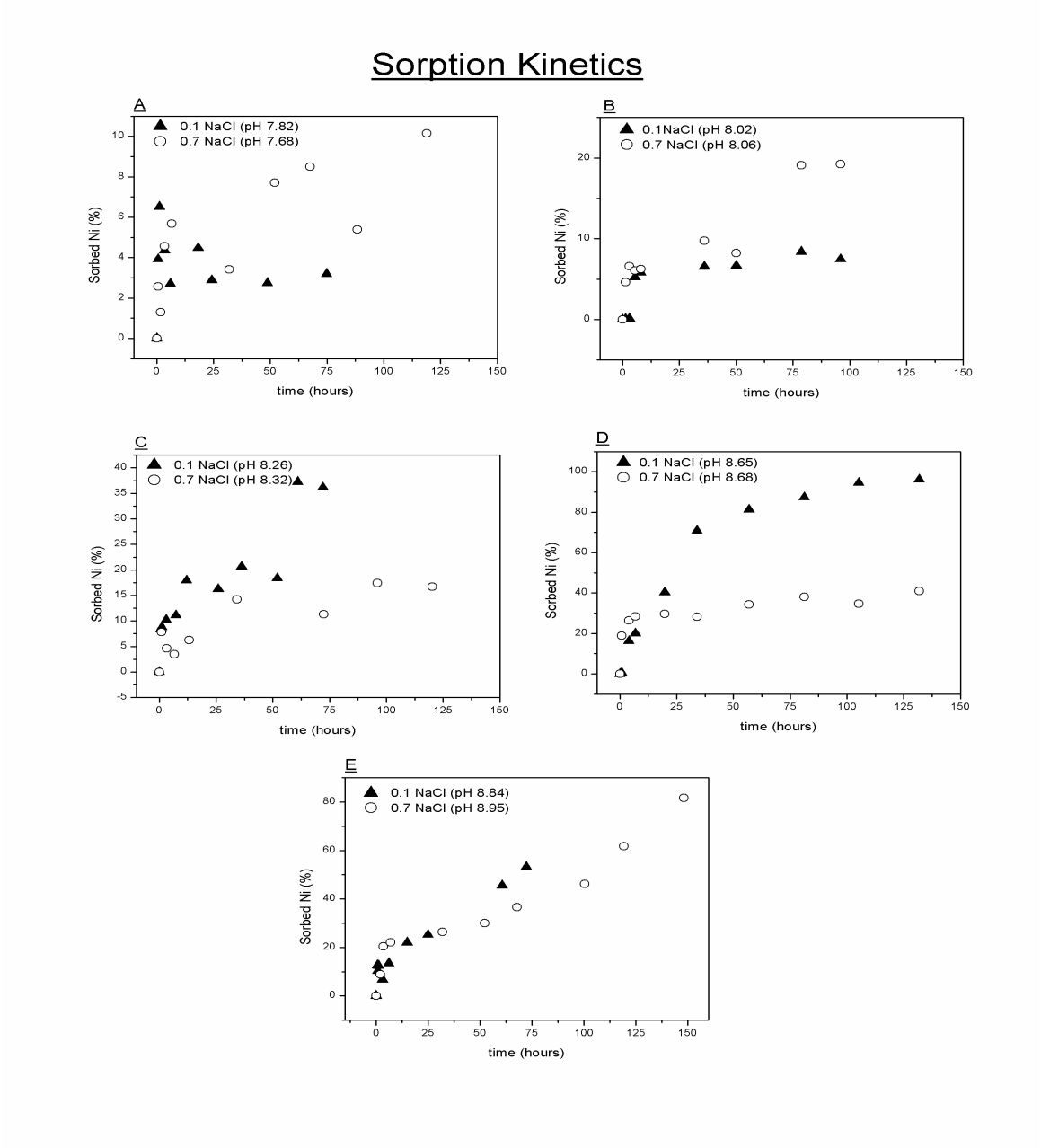

Figure 2.4- Each graph (A, B, C, D and E) represents the fractional Ni sorption (adsorption followed by either equilibrium or co-precipitation) on calcite as a function of time in solutions of various pH (ranging from 7.65-8.95). The triangles (▲) and circles (○) represent, respectively, the data obtained from the experiments carried out at ~25°C in calcite-equilibrated 0.1 M and 0.7 M NaCl solutions.

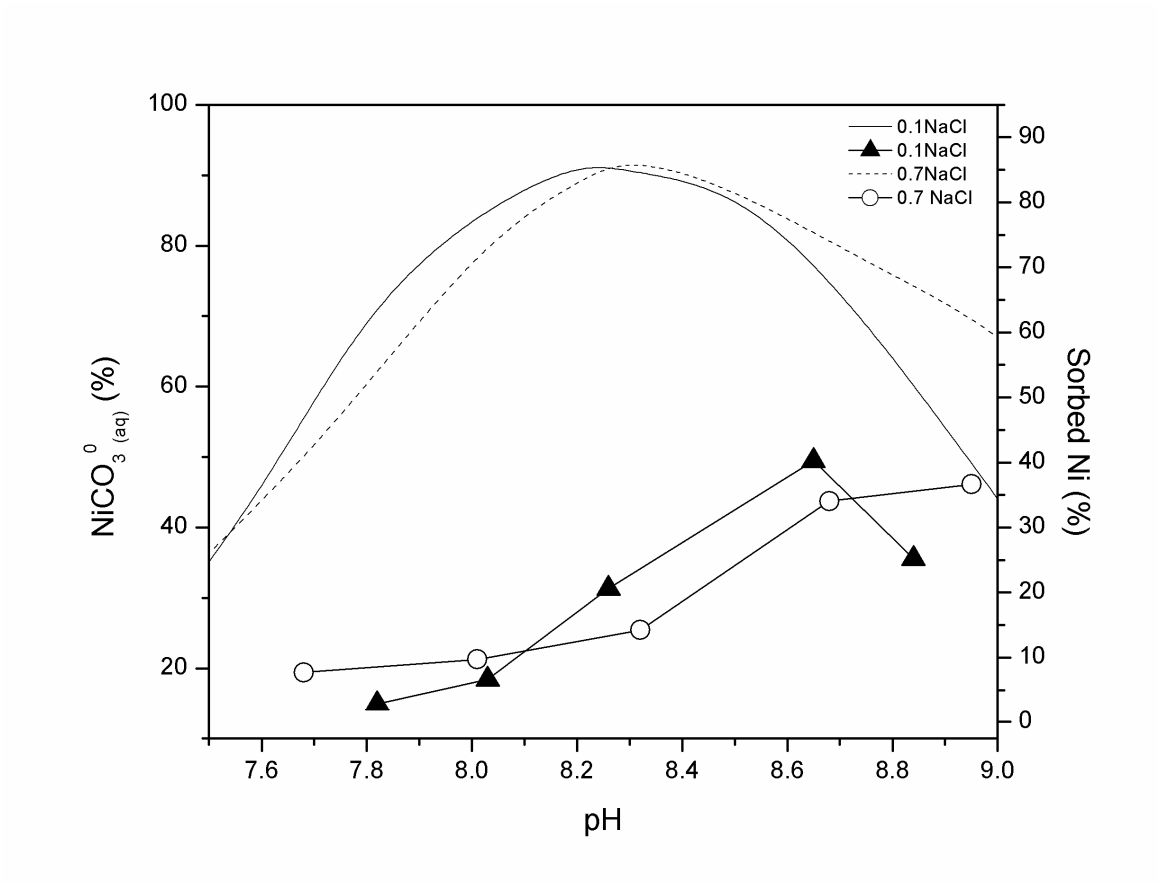

Figure 2.5- Based on the data obtained during the kinetic experiments, the fraction of adsorbed Ni from 0.1 M (▲) and 0.7 M (○) NaCl solutions after 24 hours of reaction was extracted and plotted over the same pH range (7.52-8.95). The relative abundance of the $NiCO_3^0{}_{(aq)}$ complex in the 0.1 M (---) and 0.7 M NaCl (—) solutions is overlaid.

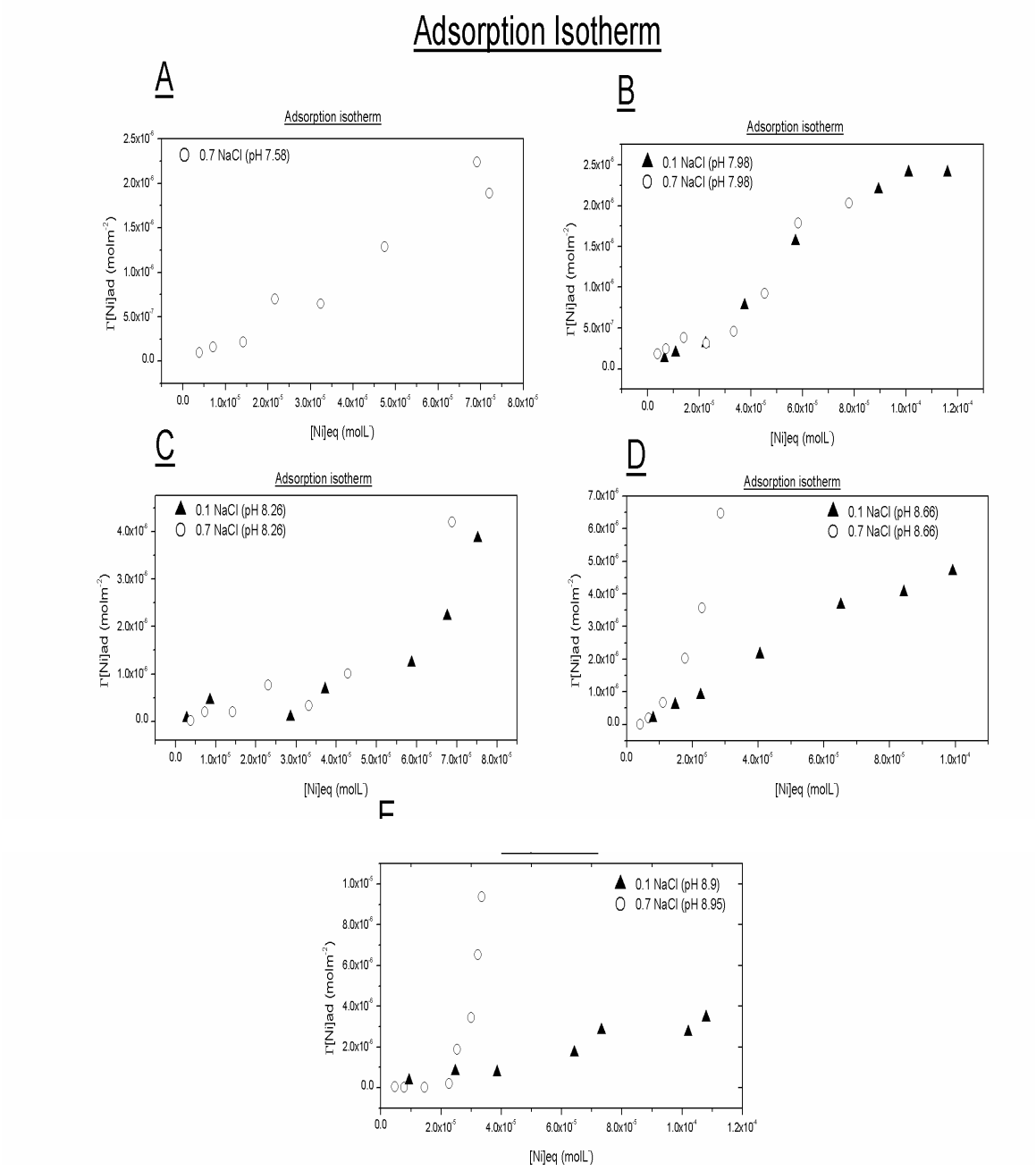

Figure 2.6- Adsorption isotherms. The graphs A, B, C, D and E represent the relationship between the bulk aqueous Ni concentration ([Ni]eq) as a function of the adsorption density (i.e. mol of adsorbed Ni per m^2). Each graph represents a distinct system with respect to solution pH (ranging from 7.58 to 8.95) and electrolyte solution concentration 0.1 M (▲) and 0.7 M (○) NaCl.

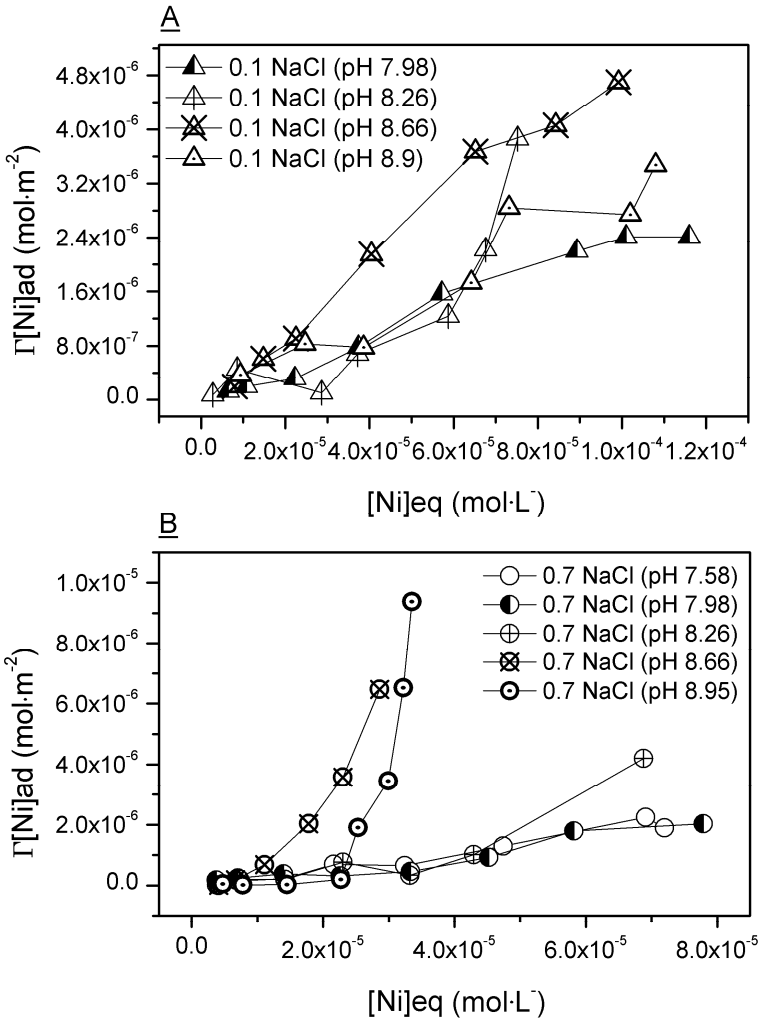

Figure 2.7- Graphs A and B are a compilation of the adsorption isotherms data obtained in, respectively, the 0.1 M and 0.7 M NaCl solutions at different pH values (ranging from 7.58 to 8.95). Each graph represents the relationship between the bulk aqueous Ni concentration ($[Ni]_{eq}$) as a function of the adsorption density (i.e. mol of adsorbed Ni per m^2) with respect to solution pH (ranging from 7.58 to 8.95) and solution ionic strength.

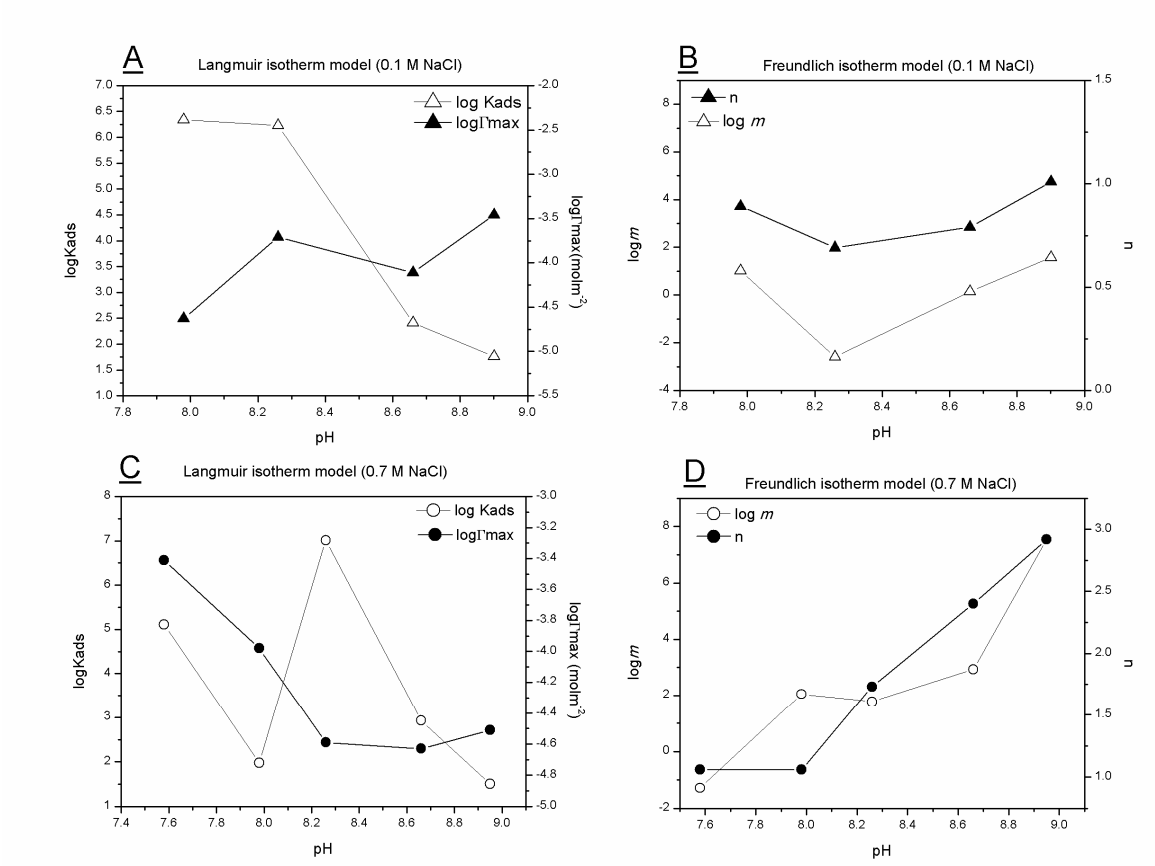

Figure 2.8- The adsorption equilibrium constant and maximum adsorption capacity (K_{ads} and Γ_{max}, respectively) derived from the Langmuir model plotted as a function of pH in calcite-equilibrated 0.1 M (graph A) and 0.7 M (graph C) NaCl solutions. The measure of the non-linearity (n) and the Freundlich adsorption constant (m) were plotted as a function of pH for the 0.1 M (graph B) and 0.7 M (graph D) NaCl solutions.

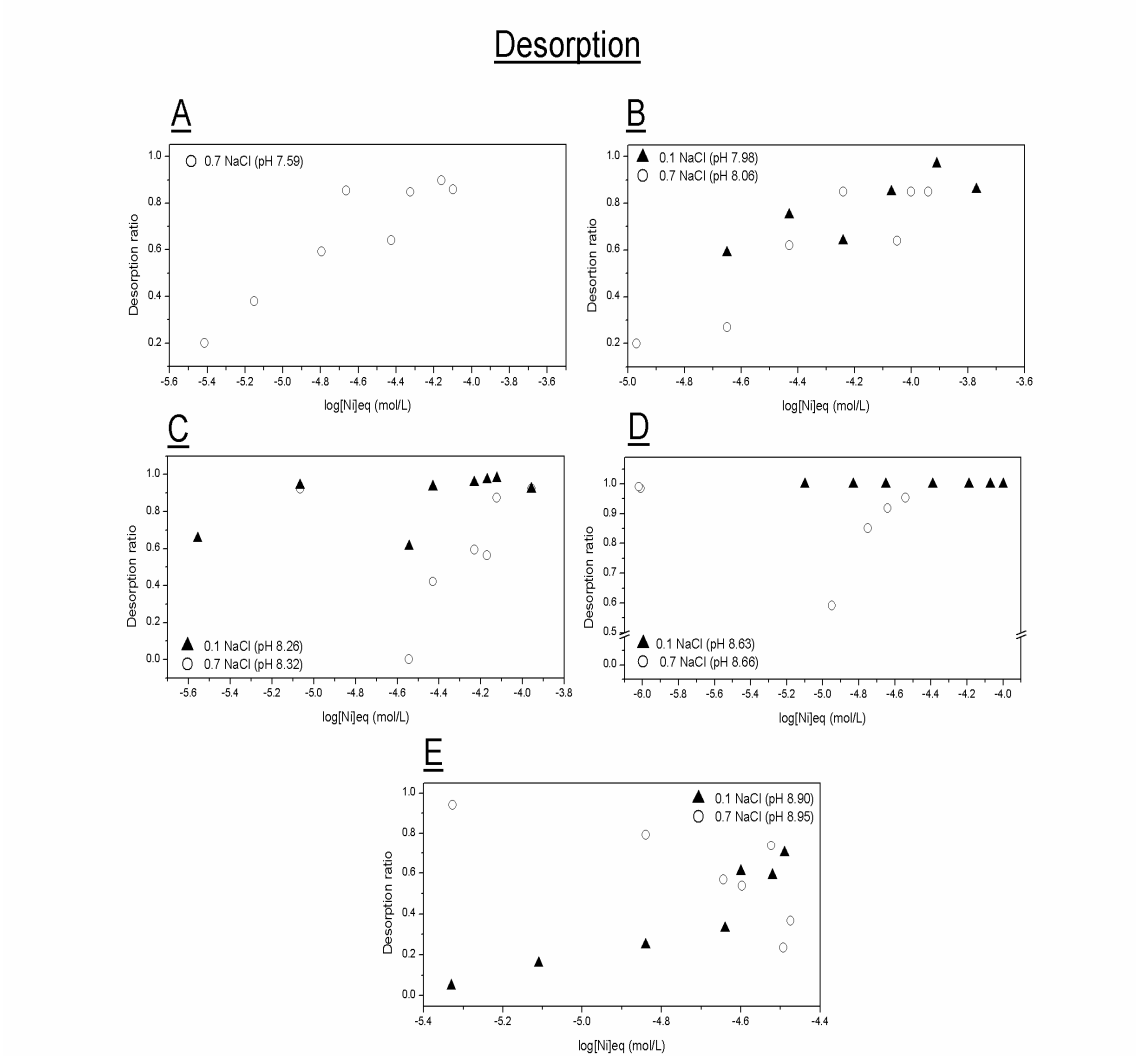

Figure 2.9 – Graphs A, B, C, D and E represent the Ni desorption from the calcite surface as a function of the bulk Ni concentration ($[Ni]_{eq}$) in solution during the adsorption isotherm experiments. Each graph represents a solution with different pH value, ranging from 7.59-8.95. The smaller the ratio, the greater is the tendency of Ni to undergo desorption. The triangles (▲) and circles (○) represent, respectively, the data obtained from the experiments carried out (~25°C) in calcite-equilibrated 0.1 M and 0.7 M NaCl solutions.

Table 2.1- Numerical data used to produce graphs in figure 2.9. Table 2.1A is a compilation of data obtained in 0.1M NaCl solutions and Table 2.1B of the data acquired in 0.7M NaCl solutions.

A

	Langmuir (0.1M NaCl)			Freundlich (0.1M NaCl)		
pH	log K_{ads}	Log Γ_{max} (mol m^{-2})	R^2	*m*	n	R^2
7.98	6.34	-4.63	0.98	1.01	0.89	0.83
8.26	6.23	-3.71	0.83	-2.6	0.69	0.92
8.66	2.41	-4.11	0.95	0.15	0.79	0.98
8.90	1.76	-3.46	0.90	1.57	1.01	0.92

B

	Langmuir (0.7M NaCl)			Freundlich (0.7M NaCl)		
pH	log K_{ads}	Log Γ_{max} (mol m^{-2})	R^2	*m*	n	R^2
7.58	5.11	-3.41	0.99	-1.28	1.06	0.99
7.98	1.98	-3.98	0.97	2.05	1.06	0.83
8.26	7.01	-4.59	0.84	1.77	1.73	0.85
8.66	2.93	-4.63	0.97	2.93	2.4	1.00
8.95	1.51	-4.51	0.98	7.55	2.92	0.87

2.6-References

Ball, J.W. and Nordstrom, D.K. (1991). User's manual for WATEQ4F, with revised thermodynamic data base and test cases for calculating speciation of major, trace and redox elements in natural waters. U.S. Geological Survey, Open-File Report 91- 183; 189 pp.

Belova, D. A., Lakshtanov, L. Z., *et al.* (2008). Experimental study of Ni adsorption on chalk: preliminary results. Mineral Magazine **72**(1): 377-379.

Brown, G. M. and Gu, B. (2006). The chemistry of perchlorate in the environment. In: Gu, B. and Coates, J. D., (Editors). Perchlorate: Environmental Occurrence, Interaction and Treatment. New York, Springer: 17-42.

Davis, J. A., Fuller, C. C., *et al.* (1987). A model for trace metal sorption processes at the calcite surface: Adsorption of Cd^{2+} and subsequent solid solution formation. Geochimica et Cosmochimica Acta **51**(6): 1477-1490.

Davis, J. A. and Kent, D. B. (1990). Surface complexation modeling in aqueous geochemistry. Reviews in Mineralogy and Geochemistry **23**(1): 177-260.

Denkhaus, E. and Salnikow, K. (2002). Nickel essentiality, toxicity, and carcinogenicity. Critical Reviews in Oncology/Hematology **42**(1): 35-56.

Dzombak, D.A. and Morel, F.M.M. (1990). Surface Complexation Modeling: Hydrous Ferric Oxide. New York, John Willey. 365 pp.

Green-Pedersen, H., Jensen, B. T., *et al.* (1997). Nickel adsorption on MnO_2, $Fe(OH)_3$, montmorillonite, humic acid and calcite: A comparative study. Environmental Technology **18**: 807-815.

Goldberg, S., Criscenti, L. J., *et al.* (2007). Adsorption desorption processes in subsurface reactive transport modeling. Vadose Zone Journal **6:** 407-435

Guillard, D. and Lewis, A. E. (2001). Nickel carbonate precipitation in a fluidized-bed reactor. Industrial & Engineering Chemistry Research **40**(23): 5564-5569.

Hoffmann, U. and Stipp, S. L. S. (2001). The behavior of Ni^{2+} on calcite surfaces. Geochimica et Cosmochimica Acta **65**(22): 4131-4139.

Honeyman B.D. and Leckie, O. J. (1986). Macroscopic partitioning coefficients for metal ion adsorption. In: Davis, J. A. and Hayes, K. F., (Editors). Geochemical Processes at Mineral Surfaces. Washington, D.C, American Chemical Society **323:** 162-190.

Jenne, E. A. (1998). Adsorption of metals by geomedia: Data analysis, modeling, controlling factors, and related issues. In: Jenne, E. A., (Editor). Adsorption of Metals by Geomedia. San Diego, Academic Press**:** 1-73.

Kowacz, M., Prieto, M., *et al.* (2010). Kinetics of crystal nucleation in ionic solutions: Electrostatics and hydration forces. Geochimica et Cosmochimica Acta **74**(2): 469-481.

Lakshtanov, L. Z. and Stipp, S. L. S. (2007). Experimental study of nickel(II) interaction with calcite: Adsorption and coprecipitation. Geochimica et Cosmochimica Acta **71**(15): 3686-3697.

Madsen, L. (2006). Calcite surface charge. In: Sumasundaran, P. and Hubbard, A., (Editors). Encyclopaedia of Surface and Colloid Science. 2nd edition. New York, Taylor and Francis: 1084-1096.

Mattigod, S., Rai, D., *et al.* (1997). Solubility and solubility product of crystalline $Ni(OH)_2$. Journal of Solution Chemistry **26**(4): 391-403.

McBride, M. B. (1997). A critique of diffuse double layer model applied to colloid and surface chemistry. Clays and Clay Minerals. **45**, 598-608.

McBride, M. B. (1979). Chemisorption and Precipitation of Mn^{2+} at $CaCO_3$ Surfaces. Soil Science Society America. J. **43**(4): 693-698.

Merkel, B. L. and Planer-Friedrich, D.K. (2008). Groundwater geochemistry: a practical guide to modelling of natural and contaminated aquatic systems. Nordstrom, D. K., (Editor). 2nd Edition. Berlin, Springer Heidelberg. 238pp.

Morse, J.W., Mackenzie, F.T. (1990). Geochemistry of Sedimentary Carbonates. In: Developments in Sedimentology **48.** New York, Elsevier. 707 pp.

Morse, J. W., Arvidson, R. S., *et al.* (2007). Calcium carbonate formation and dissolution. Chemical Reviews **107**(2): 342-381.

Moulin, P. and Roques, H. (2003). Zeta potential measurement of calcium carbonate. Journal of Colloid and Interface Science **261**(1): 115-126.

Mucci, A. (1986). Growth kinetics and composition of magnesian calcite overgrowths precipitated from seawater: quantitative influence of orthophosphate ions. Geochimica et Cosmochimica Acta **50**(10): 2255-2265.

Neilson, G.W. and Enderby, J.E. (1978). The hydration of Ni^{2+} in aqueous solutions. Journal of Physics C: Solid State Physics. **11** (L): 625.

Nieminen, T.M., Ukonmaanaho, L., *et al*. (2007) Biogeochemistry of nickel and its release into the environment. In: Sigel, A., Sigel, H. and Sigel, R. K. O., (Editors). Metal Ions in Life Sciences. New York, Wiley. **2:** 1–30.

Ödegaard-Jensen, A., Ekberg, C., *et al.* (2004). LJUNGSKILE: a program for assessing uncertainties in speciation calculations. Talanta **63**(4): 907-916.

Parkhurst, D.L and Apello, C. A. J. (1999). User's guide to PHREEQC (version 2) – A computer program for speciation, batch-reaction, one dimensional transport, and inverse geochemcal calculations. Water Resources Investigations Report. U.S. Geological Survey 99-4259. 143pp.

Pokrovsky, O. S., Mielczarski, J. A., *et al.* (2000). Surface speciation models of calcite and dolomite/aqueous solution interfaces and their spectroscopic evaluation. Langmuir **16**(6): 2677-2688.

Reeder, R. J. (1983). Crystal chemistry of the rhombohedral carbonates. In: Reeder, R. J., (Editor). Carbonates: Mineralogy and Chemistry. Reviews in Mineralogy. Washington, Mineralogical Society of America **2:** 1-48.

Reeder, R. J., Schoonen, M. A. A., *et al.* (2006). Metal speciation and its role in bioaccessibility and bioavailability. Reviews in Mineralogy and Geochemistry **64**(1): 59-113.

Román-Ross, G., Cuello, G. J., *et al.* (2006). Arsenite sorption and co-precipitation with calcite. Chemical Geology **233**(3-4): 328-336.

Rouff, A., Reeder, R., *et al.* (2002). Pb (II) Sorption with calcite: A radiotracer study. Aquatic Geochemistry **8**(4): 203-228.

Rouff, A. A., Reeder, R. J., *et al.* (2005). Electrolyte and pH effects on Pb(II)-calcite sorption processes: the role of the $PbCO^{0}_{3(aq)}$ complex. Journal of Colloid and Interface Science **286**(1): 61-67.

Sharma, Y. C., Gupta, G. S., *et al.* (1990). Use of wollastonite in the removal of Ni(II) from aqueous solutions. Water, Air, & Soil Pollution **49**(1): 69-79.

Sposito, G. (1986). On distinguishing adsorption from surface precipitation. In: Davis, J. A. and Hayes, K. F., (Editors). Geochemical Processes at Mineral Surfaces. ACS Symposium Series**.** Washington, DC, American Chemical Society. **323**: 217–228.

Stumm, W. and Morgan, J.J (1996) Aquatic Chemistry – chemical equilibria and rates in natural waters. 3rd edition. New York, Wiley-Interscience. 1005 pp.

Van Cappellen, P., Charlet, L., *et al.* (1993). A surface complexation model of the carbonate mineral-aqueous solution interface. Geochimica et Cosmochimica Acta **57**(15): 3505-3518.

Villegas-Jiménez, A., Mucci, A., *et al.* (2009). Proton/calcium ion exchange behavior of calcite. Physical Chemistry Chemical Physics **11**(39): 8895-8912.

Villegas-Jiménez, A., Mucci, A., *et al.* (2010). Acid-base behavior of the gaspeite ($NiCO_{3(s)}$) surface in NaCl solutions. Langmuir **26** (15): 12626-12639.

Wolthers M., Charlet, L., *et al*. (2004). The surface chemistry of carbonates, a new approach. In: Wanty, R. B. and Seal II, R. R., (Editors). Water-Rock Interaction. 2nd edition. London, Balkema A.A: 781–784.

Zachara, J. M., Cowan, C. E., *et al.* (1991). Sorption of divalent metals on calcite. Geochimica et Cosmochimica Acta **55**(6): 1549-1562.

Chapter 3- Final Remarks

3.1- Research summary

Adsorption, desorption and co-precipitation reactions are important processes that affect the transport of contaminants in the environment. In natural aqueous systems, adsorption and co-precipitation (sorption) are regarded as possible metal sequestration mechanisms that promote *in situ* passive remediation. Calcite is a ubiquitous mineral in the Earth's upper crust and its propensity to scavenge trace metals has been extensively investigated. With that in mind, the principal objective of this research project was to investigate Ni sorption on calcite under different chemical conditions. Hence, we analysed the net change of total Ni concentration ($[Ni]_{total}$) in aqueous solutions at a constant calcite particle loading and various pH, ionic strength and $[Ni]_{total}$ in NaCl solutions. Since no significant Ni loss was observed in calcite-free solutions, it is assumed that calcite is responsible for the Ni uptake from the aqueous phase. Since adsorption is a compulsory intermediate step for all incorporation reactions, we expected to be able to distinguish adsorption from co-precipitation through a series of experimental manipulations. Therefore, the experimental design included: geochemical equilibrium calculations to determine the saturation state of the solution with respect to possible forming/existing minerals (e.g. calcite, gaspeite and Ni-hydroxide) in the system, a description of the sorption kinetics, construction of adsorption isotherms to describe the affinity of Ni for the calcite surface through mass action relationships and, finally, the investigation of the extent of Ni sorption reversibility. From the results, a pertinent set of conclusions was drawn.

3.2- Conclusions

- Uptake kinetics revealed the dual nature of the process, whereby a significant fraction of total Ni was sorbed to the surface within the first few hours (< 24 hours) of metal-mineral contact, followed by either a plateau or slow progressive sorption with time, interpreted as metal co-precipitation or diffusion into the bulk solid phase.

- Regardless of solution ionic strength (0.1M or 0.7M NaCl), Ni(II) sorption onto the calcite surface increased with solution pH. Nevertheless, sorption was attenuated beyond pH 8.66 in 0.1M NaCl, whereas it continued to increase at higher pH in 0.7M NaCl systems.

- Ni(II) sorption, at both ionic strengths, was strongly correlated with the relative abundance of the $NiCO_3^0{}_{(aq)}$ species in solution.

- The Freundlich adsorption coefficients of non linearity (n) obtained in 0.7M NaCl were all above one (1) and systematically increased with increasing solution pH. These results may indicate that, at high Cl^- concentrations, Ni (II) adsorption on calcite is more likely to be dictated by co-precipitation. Since $NiCO_3^0{}_{(aq)}$ is weakly hydrated (due to its neutrality), the loss of its hydration shell and subsequent diffusion into the bulk solid should be facilitated in 0.7M NaCl relative to the lower ionic strength (0.1M NaCl) solutions.

- In both ionic strength solutions (0.1M and 0.7 M NaCl), Ni(II) did not readily desorb from the calcite surface, and desorption decreased as the total Ni present in solution at the onset of adsorption experiments was increased.

- In comparison with other divalent metal ions (e.g. Cd^{2+} and Zn^{2+}), over short periods of time (< 24 hours), calcite did not appear to be an effective Ni(II) scavenger (sorption did not exceed 50%).

3.3- Final recommendations

- It is important to note that the measurement of pH in this study served as an indirect approach to verify the steady state conditions in the systems investigated. Since the liquid junction potentials developed by reference electrodes are different in electrolyte solutions of dissimilar composition, future measurements should be carried out on a pH scale defined in a medium of the same composition. Hence, in reproducing this study, a TRIS buffer solution prepared in either 0.1M or 0.7M NaCl (for the buffer preparation, see Millero *et al.* 1987) should be used for electrode calibration in 0.1M or 0.7 M NaCl respectively.

- Experiments should be carried out above pH 9.0 in 0.7M NaCl to determine whether the extended stability field of $NiCO_3^0{}_{(aq)}$ in this solution favours Ni sorption on calcite, and to confirm the role of this species in controlling the interaction between Ni and the calcite surface. If so, one would expect Ni sorption to decrease above pH 9.0. Otherwise, if the fractional sorption continues to increase above this pH, enhanced Ni(II) co-precipitation could be caused by the loss of its hydration shell and subsequent diffusion into the bulk, possibly induced by the increased ionic strength in the aqueous system. Unfortunately, our systems were comprised of only two distinct ionic strengths (0.1M and 0.7M NaCl), hence it would be desirable to carry out experiments at higher ionic strengths (> 0.7M NaCl) or even in the presence of a background electrolyte

constituted of stronger ligands (e.g. SO_4^{2-}, F^-, PO_4^{3-}) to corroborate our findings. Moreover, in order to avoid the saturation of calcite adsorption sites and to determine the nature (e.g. chemical or electrostatic) of Ni(II) interactions with the calcite surface, it is imperative to carry out experiments at low Ni (< 10^{-6}M) concentrations and, thus, a radiotracer study would likely be most appropriate.

- In the absence of surface sensitive analytical methods (e.g. XAFS, EXAFS) the use of equilibrium geochemical models to calculate the solubility and aqueous speciation of the studied metal under a set of environmental conditions is critical.

- Various empirical approaches, such as the distribution coefficient and Freundlich and Langmuir isotherm equations, have been used to represent adsorption data, but they cannot account for the effects of variable chemical conditions, such as pH, alkalinity, or concentration of complexing ligands on adsorption reactions. As formulated by Sposito (1986), an adsorption isotherm equation provides no evidence as to the actual mechanism of such a process. Hence, one should stride to generate and compile the required database to develop SCMs since they can often provide insights that are not obvious from experimental observations alone. Notwithstanding, we demonstrated that, through a simple experimental design and macroscopic observations, valuable information can be extracted from our observations.

- It would be interesting to carry out column settling tests to determine the Ni sorption behaviour on the calcite surface in a continuous flow system. Results of these tests would enable engineers to develop a potential low-cost filtration protocol to remove Ni from industrial wastewaters.

3. 4-References

Millero, F. J., Hershey, J. P., *et al.* (1987). The pK* of $TRISH^+$ in Na-K-Mg-Ca-Cl-SO_4 brines-pH scales. Geochimica et Cosmochimica Acta **51**(3): 707-711.

Sposito, G. (1986). On distinguishing adsorption from surface precipitation. In: Davis, J.A. and Hayes, K.F., (Editors). Geochemical Processes at Mineral Surfaces. ACS Symposium Series**.** Washington, DC, American Chemical Society. **323**: 217–228.

APPENDIX 1- PHREEQC

Appendix 1.1 - The WATEQ approximation (Truesdell and Jones, 1974), derived from the Debye-Hückel (1925) equation, was used to estimate single ion activity coefficients (γ_i).

$$\log(\gamma_i) = [(-A \cdot Z_i^2 \cdot I^{1/2}) \cdot (1 + B \cdot \alpha_i \cdot I^{1/2})^{-1}] + b_i \cdot I$$

Where:
γ_i is the activity coefficient
Z_i is the ionic valence
I is the solution ionic strength
A and **B** are temperature-dependent parameters*
α_i (Å = 10^{-8} cm) and **bi** (L/mol) are ion-specific parameters

ion	αi (Å)	bi (L/mol)
H^+	4.78	0.24
OH^+	10.65	0.21
Na^+	4.32	0.06
Ca_2^+	4.86	0.15
Ni_2^+	5.51	0.22
Cl^-	3.71	0.01
HCO_3^-, CO_3^{2-}	5.4	0

Source: Truesdell and Jones (1974)

*For temperatures of about 25°C and water with a density of 1 g/cm^3, **A** is 0.5092 and **B** is 0.3283.

Appendix 1.2 - Total calcium concentration and alkalinity in calcite-saturated 0.1 M (solid lines) and 0.7 M NaCl (dashed lines) solutions as a function of pH and atmospheric ($pCO_2 = 10^{-3.41}$ atm) simulated in PHREEQC.

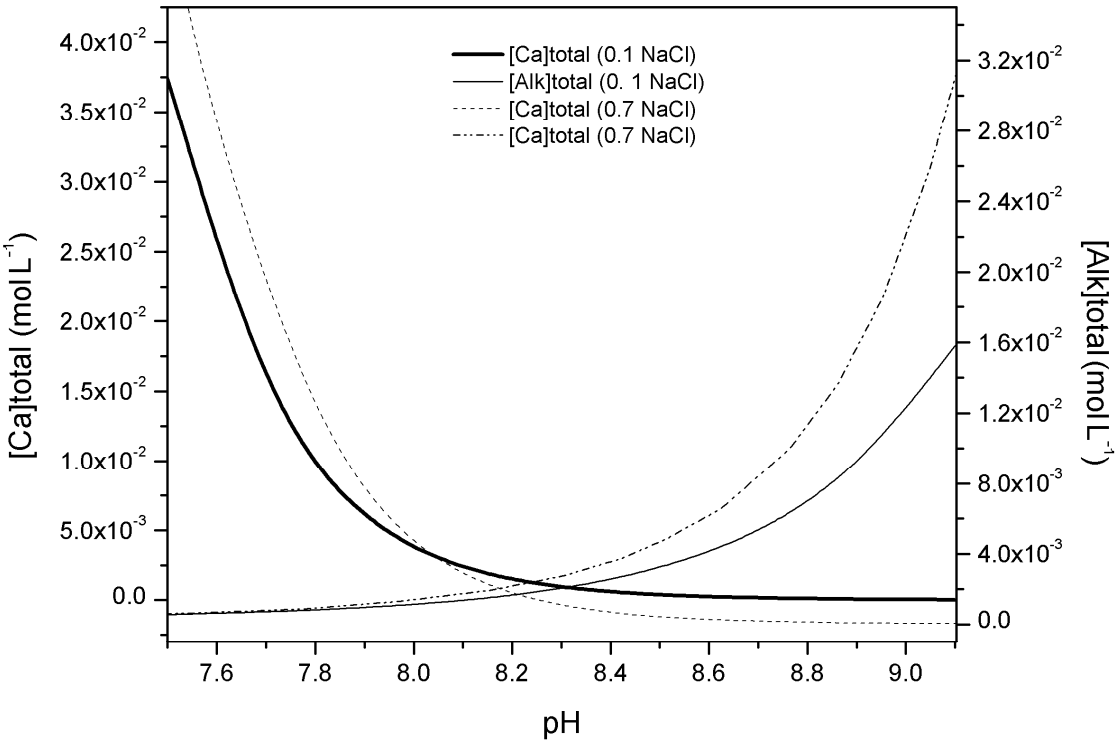

APPENDIX 2- SOLUTION BLANKS

Appendix 2.1- Solution blanks were comprised of filtered, calcite-saturated solutions of distinct NaCl concentrations (0.1M and 0.7M NaCl) and pH (7.6-8.9) to which a known amount of Ni ($[Ni]_{total}$) was added at the onset of the kinetic experiments in the absence of calcite substrate. After approximately 200 hours, the $[Ni]_{total}$ was measured to assess Ni uptake by the reactor glass walls. As reported below, the difference (Δ) in $[Ni]_{total}$ after 200 hours of reaction was less the 3%.

	0.1 M NaCl			0.7 M NaCl		
pH	$[Ni]_{initial}$ (mol/L)	$[Ni]_{final}$ (mol/L)	Δ (%)	$[Ni]_{initial}$ (mol/L)	$[Ni]_{final}$ (mol/L)	Δ (%)
7.6	N/A	N/A	N/A	1.07E-04	1.07E-04	0.1
7.8	9.65E-05	9.60E-05	0.64	N/A	N/A	N/A
8	1.52E-04	1.48E-04	2.10	1.22E-04	1.26E-04	-3.1
8.3	1.07E-04	1.06E-04	0.92	1.08E-04	1.05E-04	2.4
8.5	1.24E-04	1.26E-04	-0.96	N/A	N/A	N/A
8.9	9.14E-05	9.1E-05	0.60	N/A	N/A	N/A

where:
pH= approximate solution pH value
$[Ni]i_{nitial}$= Total Ni concentration added to solution at t_0.
$[Ni]_{final}$ = Total Ni concentration present in solution after 200 hours
Δ(%)= relative difference between Ni concentration present in the solution after 200 hours.

APPENDIX-3- KINETIC EXPERIMENTS

Appendix 3.1- Each table below contains the raw data (reaction time, total Ni concentration and fractional Ni sorption) obtained from experiments carried below pH 7.86 in calcite-saturated 0.1 M NaCl (Table A) and 0.7 M NaCl (Table B) solutions open to the atmosphere ($pCO_2=10^{-3.41}$ atm) (Table B). The calcite particle loading (5.2 $m^2\ L^{-1}$) was kept constant at all times.

A) 0.1 M NaCl (pH = 7.86. pH' = 7.82)

Time (hours)	$[Ni]_{total}$ (mol/L)	%
0	5.58E-06	0
0.62	5.42E-06	3.92
1.23	9.00E-06	6.52
3.46	6.00E-06	4.35
6.03	3.74E-06	2.71
18.34	6.20E-06	4.48
24.35	4.00E-06	2.88
48.73	3.80E-06	2.75
74.85	4.40E-06	3.19

B) 0.7 M NaCl (pH = 7.68, pH' = 7.62)

Time (hours)	$[Ni]_{total}$ (mol/L)	%
0	1.06E-05	0
0.69	1.03E-05	2.58
1.71	1.01E-05	1.29
3.43	9.55E-06	4.56
6.7	4.28E-06	5.68
31.89	1.74E-06	3.41
51.99	6.75E-06	7.71
67.64	7.67E-06	8.5
88.3	4.05E-06	5.39
119.01	9.60E-06	10.16

Where :
pH = pH value at the onset of the experiment
pH' = pH value by the end of the experiment
Time = time period over which desorption was allowed to proceed
$[Ni]_{total}$ = total Ni concentration present in solution by the end of the adsorption experiment
% = Fractional Ni sorbed on calcite after various periods of reaction

Appendix 3.2- Each table below contains the raw data (reaction time, total Ni concentration and fractional Ni sorption) obtained from experiments carried below pH 8.09 in calcite-saturated 0.1 M NaCl (Table A) and 0.7 M NaCl (Table B) solutions open to the atmosphere ($pCO_2=10^{-3.41}$ atm) (Table B). The calcite particle loading (5.2 $m^2 L^{-1}$) was kept constant at all times.

A) 0.1M NaCl (pH = 8.01, pH'= 8.02)

Time (hours)	$[Ni]_{total}$ (mol/L)	%
0.00	8.61E-05	0.00
1.23	8.55E-05	0.07
3.06	8.51E-05	0.12
5.51	8.16E-05	5.21
8.00	8.11E-05	5.81
36.06	8.05E-05	6.55
50.06	8.04E-05	6.66
78.71	7.89E-05	8.39
96.03	7.97E-05	7.47

B) 0.7M NaCl (pH = 8.09, pH'= 8.06)

Time (hours)	$[Ni]_{total}$ (mol/L)	%
0.00	8.65E-05	0.00
1.23	8.25E-05	4.63
3.06	8.08E-05	6.61
5.51	8.13E-05	6.06
8.00	8.11E-05	6.24
36.06	7.81E-05	9.73
50.06	7.94E-05	8.21
78.71	7.00E-05	19.10
96.03	6.99E-05	19.20

Where :
pH = pH value at the onset of the experiment
pH' = pH value by the end of the experiment
Time = time period over which desorption was allowed to proceed
$[Ni]_{total}$ = total Ni concentration present in solution by the end of the adsorption experiment
% = Fractional Ni sorbed on calcite after various periods of reaction

Appendix 3.3- Each table below contains the raw data (reaction time, total Ni concentration and fractional Ni sorption) obtained from experiments carried below pH 8.32 in calcite-saturated 0.1 M NaCl (Table A) and 0.7 M NaCl (Table B) solutions open to the atmosphere ($pCO_2=10^{-3.41}$ atm) (Table B). The calcite particle loading (5.2 $m^2 L^{-1}$) was kept constant at all times.

A) 0.1 M NaCl (pH 8.30, pH' = 8.26)

Time(hours)	$[Ni]_{total}$ (mol/L)	%
0.00	1.38E-04	0.00
0.75	1.15E-05	8.33
1.15	1.21E-05	8.79
3.00	1.41E-05	10.23
7.35	1.53E-05	11.10
12.00	2.47E-05	17.92
26.00	2.24E-05	16.24
36.33	2.85E-05	20.62
52.00	2.54E-05	18.37
61.00	5.14E-05	37.25
72.15	4.99E-05	36.12

B) 0.7 M NaCl (pH 8.29, pH' = 8.32)

Time(hours)	$[Ni]_{total}$ (mol/L)	%
0.00	1.08E-04	0.00
1.07	9.93E-05	7.80
3.30	1.03E-04	4.65
6.56	1.04E-04	3.48
13.13	1.01E-04	6.25
34.18	1.53E-04	14.23
72.35	1.22E-05	11.31
96.10	1.88E-05	17.44
120.20	1.80E-05	16.70

Where :
pH = pH value at the onset of the experiment
pH' = pH value by the end of the experiment
Time = time period over which desorption was allowed to proceed
$[Ni]_{total}$ = total Ni concentration present in solution by the end of the adsorption experiment
% = Fractional Ni sorbed on calcite after various periods of reaction

Appendix 3.4- Each table below contains the raw data (reaction time, total Ni concentration and fractional Ni sorption) obtained from experiments carried below pH 8.68 in calcite-saturated 0.1 M NaCl (Table A) and 0.7 M NaCl (Table B) solutions open to the atmosphere ($pCO_2=10^{-3.41}$ atm) (Table B). The calcite particle loading (5.2 $m^2 L^{-1}$) was kept constant at all times.

A) 0.1 M NaCl (pH= 8.69, pH'=8.65)

Time(hours)	$[Ni]_{total}$ (mol/L)	%
0.00	3.19E-05	0.00
0.75	3.17E-05	0.63
3.95	2.67E-05	16.26
6.90	2.55E-05	20.00
19.83	1.91E-05	40.28
33.95	9.30E-06	70.86
56.95	6.00E-06	81.21
81.21	4.02E-06	87.41
105.21	1.74E-06	94.56
131.83	1.23E-06	96.16

B) 0.7 M NaCl (pH = 8.62, pH' = 8.68)

Time(hours)	$[Ni]_{total}$ (mol/L)	%
0.00	7.14E-05	0.00
0.63	1.35E-05	18.88
3.70	1.89E-05	26.42
6.78	2.02E-05	28.33
19.65	2.12E-05	29.73
33.83	2.01E-05	28.18
56.83	2.46E-05	34.38
81.13	2.72E-05	38.08
105.31	2.48E-05	34.72
131.75	2.92E-05	40.92

Where :
pH = pH value at the onset of the experiment
pH' = pH value by the end of the experiment
Time = time period over which desorption was allowed to proceed
$[Ni]_{total}$ = total Ni concentration present in solution by the end of the adsorption experiment
% = Fractional Ni sorbed on calcite after various periods of reaction

Appendix 3.5- Each table below contains the raw data (reaction time, total Ni concentration and fractional Ni sorption) obtained from experiments carried below pH 8.95 in calcite-saturated 0.1 M NaCl (Table A) and 0.7 M NaCl (Table B) solutions open to the atmosphere ($pCO_2=10^{-3.41}$ atm) (Table B). The calcite particle loading (5.2 $m^2 L^{-1}$) was kept constant at all times.

A) 0.1 M NaCl (pH = 8.91, pH'= 8.84)

Time(hours)	$[Ni]_{total}$ (mol/L)	%
0.00	1.29E-04	0.00
0.45	1.63E-05	12.59
0.80	1.34E-05	10.32
1.08	1.62E-05	12.49
3.05	8.78E-06	6.78
6.03	1.75E-05	13.49
14.98	2.85E-05	22.03
24.87	3.27E-05	25.23
60.62	5.89E-05	45.51
72.20	6.89E-05	53.24

B) 0.7 M NaCl (pH = 8.88, pH'= 8.95)

Time(hours)	$[Ni]_{total}$ (mol/L)	%
0.00	1.11E-04	0.00
1.93	9.99E-05	8.88
3.41	1.01E-04	20.36
6.82	9.53E-05	22.00
31.96	9.03E-05	26.48
52.17	8.63E-05	29.95
67.77	7.68E-05	36.64
100.44	5.97E-05	46.21
119.28	3.52E-05	61.77
148.09	1.25E-05	81.64

Where :
pH = pH value at the onset of the experiment
pH' = pH value by the end of the experiment
Time = time period over which desorption was allowed to proceed
$[Ni]_{total}$ = total Ni concentration present in solution by the end of the adsorption experiment
% = Fractional Ni sorbed on calcite after various periods of reaction

APENDIX 4 - ADSORPTION ISOTHERM EXPERIMENTS

Appendix 4.1 - The table below contains the data obtained from experiments carried in a 0.7M NaCl solution at pH 7.58. The calcite particle loading (5.2 m^2 L^{-1}) and solution volume (100 mL) were kept constant at all times.

0.7 M NaCl (pH = 7.52; pH' = 7.58)

Time (hours)	$[Ni]_{total}$ (mol/L)	$[Ni]_{eq}$ (mol/L)	$\Gamma[Ni]_{ad}$ (mol/m^2)
22.91	4.36E-06	3.85E-06	9.83E-08
22.91	7.90E-06	7.07E-06	1.59E-07
23.38	1.53E-05	1.42E-05	2.18E-07
23.38	2.53E-05	2.16E-05	6.98E-07
23.75	3.58E-05	3.24E-05	6.47E-07
23.75	5.41E-05	4.74E-05	1.29E-06
24	8.08E-05	6.91E-05	2.24E-06
24	8.18E-05	7.20E-05	1.89E-06

pH = pH value at the onset of the experiment.
pH' = pH value by the end of the experiment.
Time = time period over which adsorption reaction was allowed to proceed.
$[Ni]_{total}$ = total Ni concentration added at the onset of adsorption experiment.
$[Ni]_{eq}$ = total Ni concentration present in solution by the end of adsorption experiment.

$\Gamma[Ni]_{ad}$ = Ni adsorption density.
Where: $\Gamma[Ni]_{ad} = (([Ni]_{total} - [Ni]_{eq}) \bullet 0.1\ L) \bullet (0.52\ m^2)^{-1}$

Appendix 4.1.A - The reciprocal and logarithmic form of the data presented in appendix 4.2 were plotted as Langmuir and Freundlich isotherms.

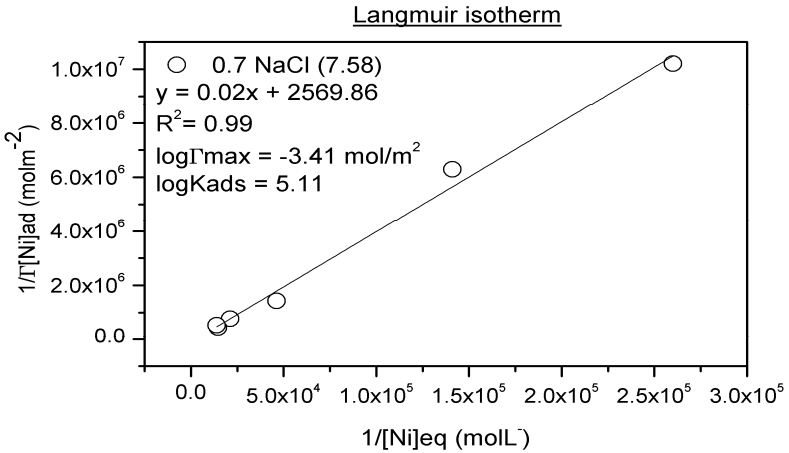

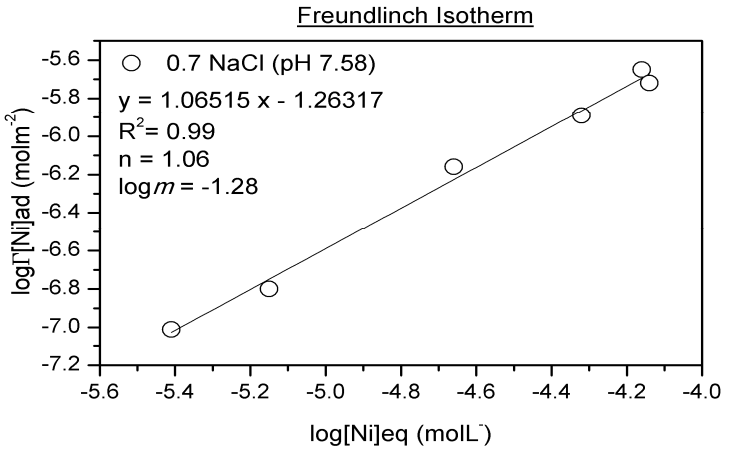

Appendix 4.2 - The table below contains the data obtained from experiments carried in a 0.1M NaCl solution at pH 7.98. The calcite particle loading (5.2 m^2 L^{-1}) and solution volume (100 mL) were kept constant at all times.

0.1 M NaCl (pH = 7.94; pH' = 7.98)

Time (hours)	$[Ni]_{total}$ (mol/L)	$[Ni]_{eq}$ (mol/L)	$\Gamma[Ni]_{ad}$ (mol/m^2)
25.35	7.11E-06	6.44E-06	1.30E-07
25.35	1.18E-05	1.08E-05	1.97E-07
26.66	2.39E-05	2.23E-05	3.13E-07
26.66	4.14E-05	3.74E-05	7.78E-07
27.23	6.53E-05	5.72E-05	1.57E-06
27.16	1.01E-04	8.93E-05	2.20E-06
27.6	1.14E-04	1.01E-04	2.41E-06
27.6	1.29E-04	1.16E-04	2.41E-06

pH = pH value at the onset of the experiment.
pH' = pH value by the end of the experiment.
Time = time period over which adsorption reaction was allowed to proceed.
$[Ni]_{total}$ = total Ni concentration added at the onset of adsorption experiment.
$[Ni]_{eq}$ = total Ni concentration present in solution by the end of adsorption experiment.

$\Gamma[Ni]_{ad}$ = Ni adsorption density.
Where: $\Gamma[Ni]_{ad} = (([Ni]_{total} - [Ni]_{eq}) \bullet 0.1\ L) \bullet (0.52\ m^2)^{-1}$

Appendix 4.2.A - The reciprocal and logarithmic form of the data presented in appendix 4.2 were plotted as Langmuir and Freundlich isotherms.

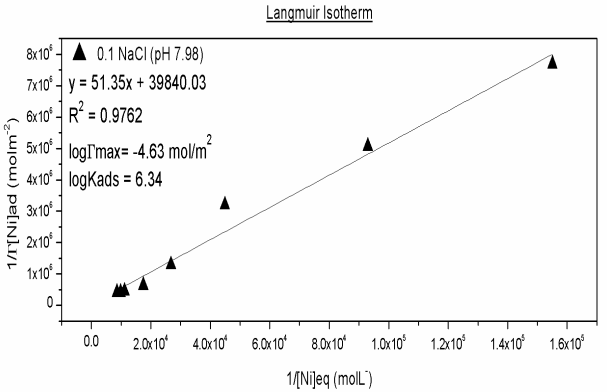

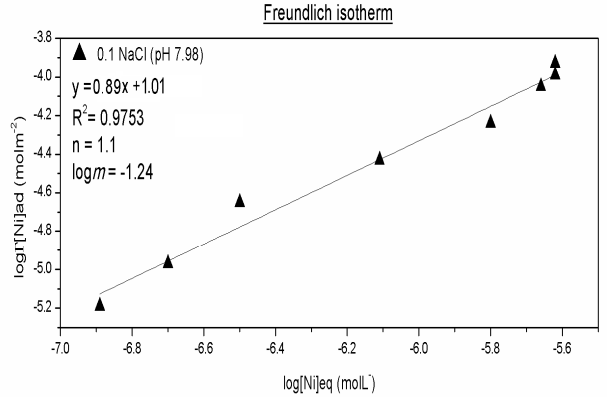

Appendix 4.3 - The table below contains the data obtained from experiments carried in a 0.7M NaCl solution at pH 7.98. The calcite particle loading (5.2 m^2 L^{-1}) and solution volume (100 mL) were kept constant at all times.

0.7 M NaCl (pH = 7.96; pH' = 7.98)

Time (hours)	$[Ni]_{total}$ (mol/L)	$[Ni]_{eq}$ (mol/L)	$\Gamma[Ni]_{ad}$ (mol/m^2)
29.36	4.70E-06	9.37E-07	1.80E-07
29.36	8.31E-06	1.29E-06	2.49E-07
29.56	1.60E-05	1.98E-06	3.80E-07
29.56	2.43E-05	1.65E-06	3.18E-07
29.7	3.57E-05	2.37E-06	4.55E-07
29.7*	5.01E-05	4.80E-06	9.24E-07
29.85*	6.75E-05	9.28E-06	1.79E-06
29.85*	8.84E-05	1.05E-05	2.03E-06

pH = pH value at the onset of the experiment.
pH' = pH value by the end of the experiment.
Time = time period over which adsorption reaction was allowed to proceed.
$[Ni]_{total}$ = total Ni concentration added at the onset of adsorption experiment.
$[Ni]_{eq}$ = total Ni concentration present in solution by the end of adsorption experiment.

$\Gamma[Ni]_{ad}$ = Ni adsorption density.
Where: $\Gamma[Ni]_{ad} = (([Ni]_{total} - [Ni]_{eq}) \bullet 0.1\ L) \bullet (0.52\ m^2)^{-1}$
*Data excluded from the regression analysis in the Langmuir isotherm

Appendix 4.3.A - The reciprocal and logarithmic form of the data presented in appendix 4.3 were plotted as Langmuir and Freundlich isotherms.

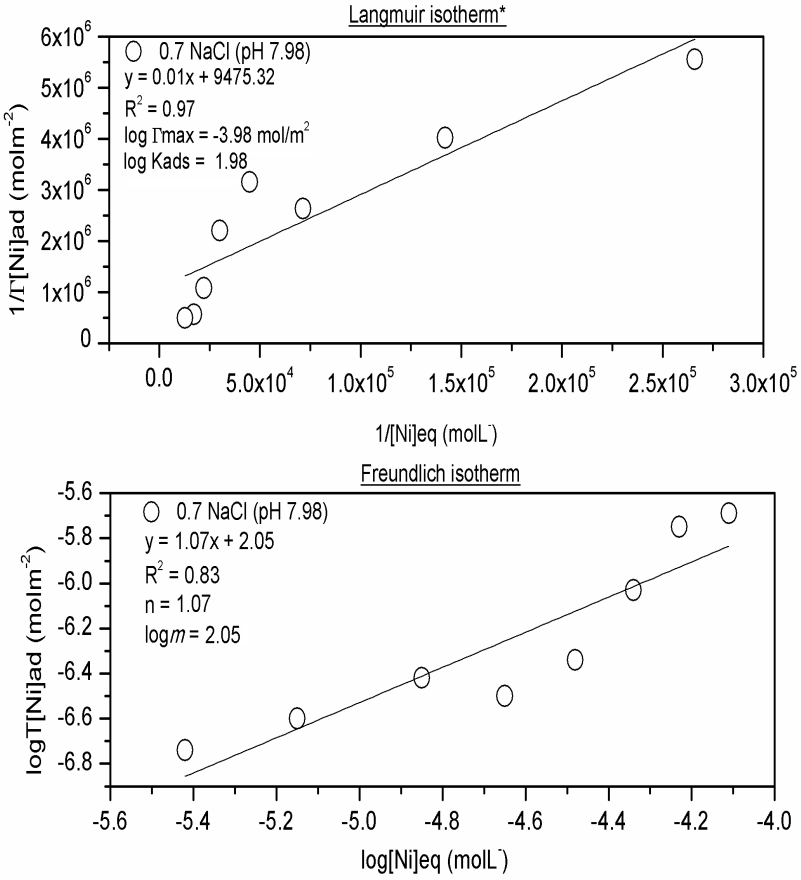

Appendix 4.4 - The table below contains the data obtained from experiments carried in a 0.1M NaCl solution at pH 8.26. The calcite particle loading (5.2 m^2 L^{-1}) and solution volume (100 mL) were kept constant at all times.

0.1 M NaCl (pH = 8.36; pH' = 8.26)

Time (hours)	$[Ni]_{total}$ (mol/L)	$[Ni]_{eq}$ (mol/L)	$\Gamma[Ni]_{ad}$ (mol/m^2)
26.16	3.15E-06	3.75E-07	7.21E-08
26.33*	1.10E-05	2.37E-06	4.55E-07
26.5*	2.91E-05	5.28E-07	1.02E-07
26.66	4.07E-05	3.54E-06	6.81E-07
26.83	6.51E-05	6.42E-06	1.24E-06
27	7.91E-05	1.16E-05	2.22E-06
27.16	9.53E-05	2.01E-05	3.86E-06
27.33*	1.15E-04	4.80E-06	9.24E-07

pH = pH value at the onset of the experiment.
pH' = pH value by the end of the experiment.
Time = time period over which adsorption reaction was allowed to proceed.
$[Ni]_{total}$ = total Ni concentration added at the onset of adsorption experiment.
$[Ni]_{eq}$ = total Ni concentration present in solution by the end of adsorption experiment.

$\Gamma[Ni]_{ad}$ = Ni adsorption density.
Where: $\Gamma[Ni]_{ad} = (([Ni]_{total} - [Ni]_{eq}) \bullet 0.1\ L) \bullet (0.52\ m^2)^{-1}$
*Data excluded from the regression analysis in the Langmuir and Freundlich isotherms.

Appendix 4.4.A - The reciprocal and logarithmic form of the data presented in appendix 4.4 were plotted as Langmuir and Freundlich isotherms.

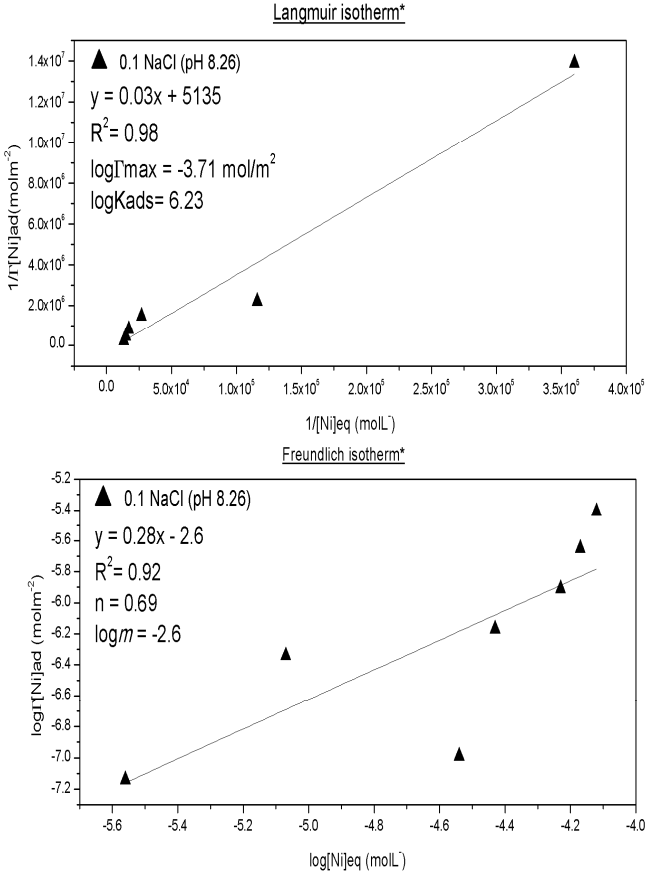

Appendix 4.5 - The table below contains the data obtained from experiments carried in a 0.7 M NaCl solution at pH 8.26. The calcite particle loading (5.2 m^2 L^{-1}) and solution volume (100 mL) were kept constant at all times.

0.7 M NaCl (pH = 8.30; pH' = 8.26)

Time (hours)	$[Ni]_{total}$ (mol/L)	$[Ni]_{eq}$ (mol/L)	$\Gamma[Ni]_{ad}$ (mol/m^2)
29.41	3.87E-06	8.52E-08	1.64E-08
29.41	8.31E-06	1.02E-06	1.97E-07
29.58	1.52E-05	1.04E-06	2.00E-07
29.58	2.70E-05	3.95E-06	7.60E-07
29.83	3.50E-05	1.72E-06	3.31E-07
29.83	4.82E-05	5.23E-06	1.01E-06
30.08	9.06E-05	2.18E-05	4.20E-06
30.08	8.93E-05	3.43E-05	6.60E-06

pH = pH value at the onset of the experiment.
pH' = pH value by the end of the experiment.
Time = time period over which adsorption reaction was allowed to proceed.
$[Ni]_{total}$ = total Ni concentration added at the onset of adsorption experiment.
$[Ni]_{eq}$ = total Ni concentration present in solution by the end of adsorption experiment.

$\Gamma[Ni]_{ad}$ = Ni adsorption density.
Where: $\Gamma[Ni]_{ad} = (([Ni]_{total} - [Ni]_{eq}) \bullet 0.1\ L) \bullet (0.52\ m^2)^{-1}$

Appendix 4.5.A - The reciprocal and logarithmic form of the data presented in appendix 4.5 were plotted as Langmuir and Freundlich isotherms.

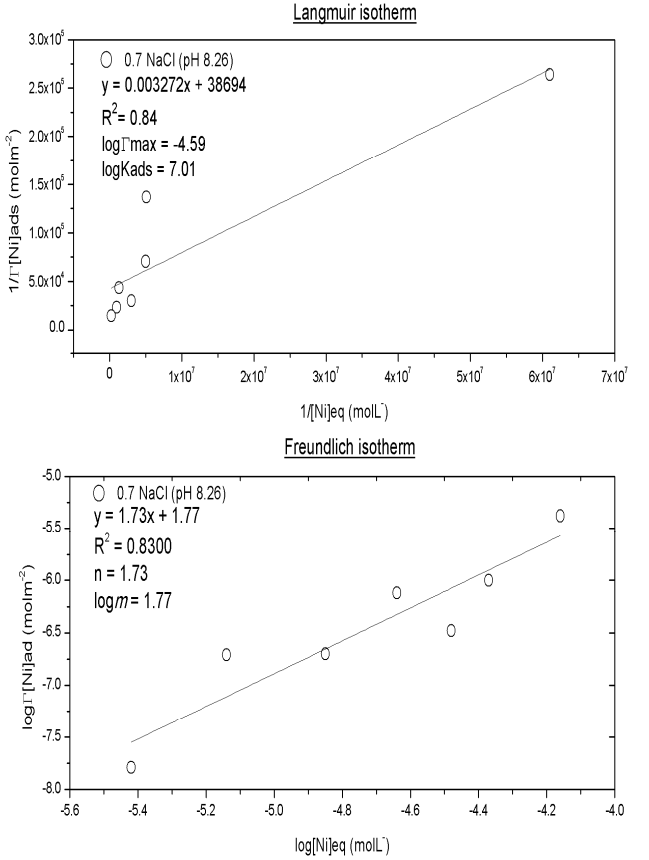

Appendix 4.6 - The table below contains the data obtained from experiments carried in a 0.1 M NaCl solution at pH 8.66. The calcite particle loading (5.2 m^2 L^{-1}) and solution volume (100 mL) were kept constant at all times.

0.1 M NaCl (pH = 8.62; pH' = 8.66)

Time (hours)	$[Ni]_{total}$ (mol/L)	$[Ni]_{eq}$ (mol/L)	$\Gamma[Ni]_{ad}$ (mol/m^2)
32.2	9.05E-06	1.02E-06	1.97E-07
32.2	1.80E-05	3.17E-06	6.09E-07
32.66	2.73E-05	4.72E-06	9.07E-07
32.66	5.17E-05	1.12E-05	2.15E-06
32.86	8.43E-05	1.91E-05	3.67E-06
32.83	1.05E-04	2.11E-05	4.06E-06
33	1.24E-04	2.44E-05	4.70E-06

pH = pH value at the onset of the experiment.
pH' = pH value by the end of the experiment.
Time = time period over which adsorption reaction was allowed to proceed.
$[Ni]_{total}$ = total Ni concentration added at the onset of adsorption experiment.
$[Ni]_{eq}$ = total Ni concentration present in solution by the end of adsorption experiment.

$\Gamma[Ni]_{ad}$ = Ni adsorption density.
Where: $\Gamma[Ni]_{ad} = (([Ni]_{total} - [Ni]_{eq}) \bullet 0.1\ L) \bullet (0.52\ m^2)^{-1}$

Appendix 4.6.A - The reciprocal and logarithmic form of the data presented in appendix 4.6 were plotted as Langmuir and Freundlich isotherms.

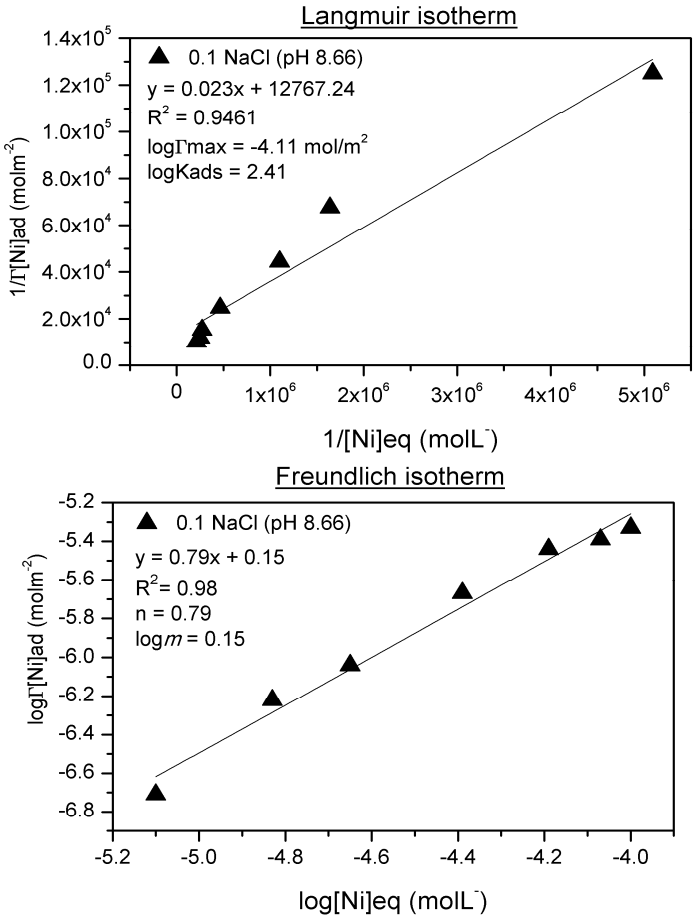

Appendix 4.7 - The table below contains the data obtained from experiments carried in a 0.7 M NaCl solution at pH 8.66. The calcite particle loading (5.2 m^2 L^{-1}) and solution volume (100 mL) were kept constant at all times.

0.7 M NaCl (pH = 8.65; pH' = 8.66)

Time (hours)	$[Ni]_{total}$ (mol/L)	$[Ni]_{eq}$ (mol/L)	$\Gamma[Ni]_{ad}$ (mol/m^2)
31.38*	4.12E-06	3.41E-08	6.55E-09
31.38	7.66E-06	9.80E-07	1.88E-07
31.48	1.47E-05	3.54E-06	6.81E-07
31.48	2.83E-05	1.05E-05	2.03E-06
31.65	4.17E-05	1.86E-05	3.58E-06
31.73	6.23E-05	3.37E-05	6.47E-06
31.83*	6.55E-05	6.45E-05	1.24E-05

pH = pH value at the onset of the experiment.
pH' = pH value by the end of the experiment.
Time = time period over which adsorption reaction was allowed to proceed.
$[Ni]_{total}$ = total Ni concentration added at the onset of adsorption experiment.
$[Ni]_{eq}$ = total Ni concentration present in solution by the end of adsorption experiment.

$\Gamma[Ni]_{ad}$ = Ni adsorption density.
Where: $\Gamma[Ni]_{ad} = (([Ni]_{total} - [Ni]_{eq}) \bullet 0.1\ L) \bullet (0.52\ m^2)^{-1}$
*Data excluded from the regression analysis in the Langmuir and Freundlich isotherms.

Appendix 4.7.A - The reciprocal and logarithmic form of the data presented in appendix 4.7 were plotted as Langmuir and Freundlich isotherms.

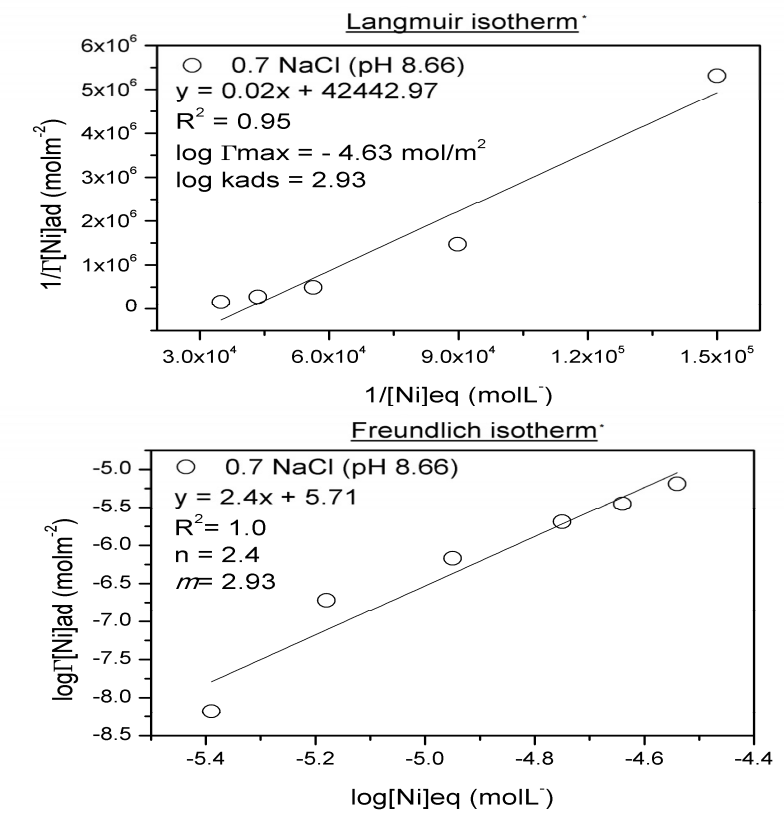

Appendix 4.8 - The table below contains the data obtained from experiments carried in a 0.1 M NaCl solution at pH 8.90. The calcite particle loading (5.2 m^2 L^{-1}) and solution volume (100 mL) were kept constant at all times.

0.1 M NaCl (pH = 8.88; pH' = 8.90)

Time (hours)	$[Ni]_{total}$ (mol/L)	$[Ni]_{eq}$ (mol/L)	$\Gamma[Ni]_{ad}$ (mol/m^2)
27.16	9.32E-06	1.91E-06	3.67E-07
27.16	2.47E-05	4.31E-06	8.29E-07
27.33	3.86E-05	4.04E-06	7.76E-07
27.33	6.42E-05	8.98E-06	1.73E-06
27.5	7.32E-05	1.48E-05	2.84E-06
27.5	1.02E-04	1.43E-05	2.74E-06
27.58	1.08E-04	1.80E-05	3.47E-06

pH = pH value at the onset of the experiment.
pH' = pH value by the end of the experiment.
Time = time period over which adsorption reaction was allowed to proceed.
$[Ni]_{total}$ = total Ni concentration added at the onset of adsorption experiment.
$[Ni]_{eq}$ = total Ni concentration present in solution by the end of adsorption experiment.

$\Gamma[Ni]_{ad}$ = Ni adsorption density.
Where: $\Gamma[Ni]_{ad} = (([Ni]_{total} - [Ni]_{eq}) \bullet 0.1\ L) \bullet (0.52\ m^2)^{-1}$

Appendix 4.8.A - The reciprocal and logarithmic form of the data presented in appendix 4.8 were plotted as Langmuir and Freundlich isotherms.

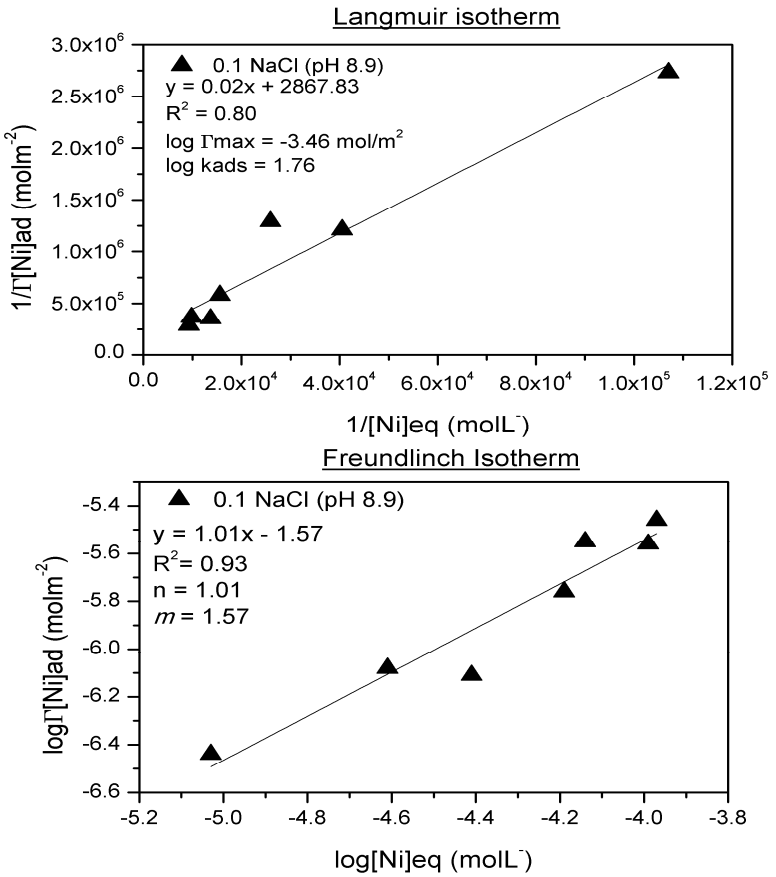

Appendix 4.9 - The table below contains the data obtained from experiments carried in a 0.7 M NaCl solution at pH 8.95. The calcite particle loading (5.2 m^2 L^{-1}) and solution volume (100 mL) were kept constant at all times.

0.7 M NaCl (pH = 8.92; pH' = 8.95)

Time (hours)	$[Ni]_{total}$ (mol/L)	$[Ni]_{eq}$ (mol/L)	$\Gamma[Ni]_{ad}$ (mol/m^2)
25.36	5.01E-06	2.98E-07	5.73E-08
25.36	7.87E-06	9.37E-08	1.80E-08
25.83	1.47E-05	1.87E-07	3.60E-08
25.83	2.37E-05	1.01E-06	1.95E-07
26.25	3.52E-05	9.88E-06	1.90E-06
26.26	4.79E-05	1.79E-05	3.45E-06
26.78	6.61E-05	3.40E-05	6.53E-06

pH = pH value at the onset of the experiment.
pH' = pH value by the end of the experiment.
Time = time period over which adsorption reaction was allowed to proceed.
$[Ni]_{total}$ = total Ni concentration added at the onset of adsorption experiment.
$[Ni]_{eq}$ = total Ni concentration present in solution by the end of adsorption experiment.

$\Gamma[Ni]_{ad}$ = Ni adsorption density.
Where: $\Gamma[Ni]_{ad} = (([Ni]_{total} - [Ni]_{eq}) \bullet 0.1\ L) \bullet (0.52\ m^2)^{-1}$

Appendix 4.9.A - The reciprocal and logarithmic form of the data presented in appendix 4.9 were as Langmuir and Freundlich isotherms.

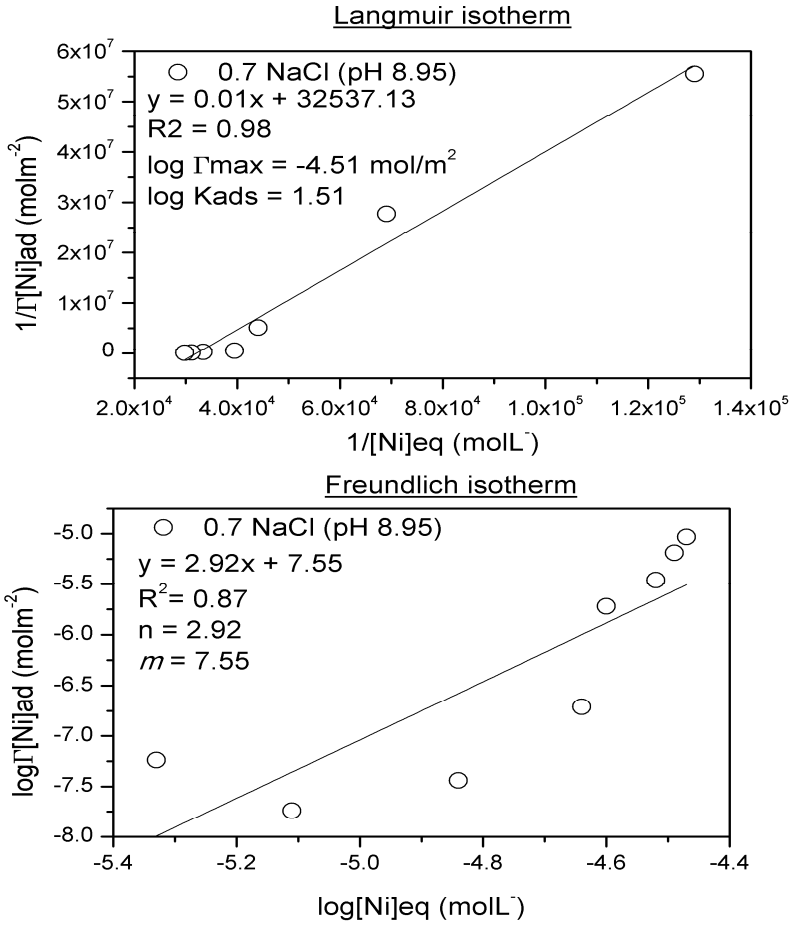

APENDIX 5- DESORPTION EXPERIMENTS

Appendix 5.1- The table below represents a compilation of the data obtained from adsorption isotherm experiments coupled with data obtained from desorption experiments carried out in 0.7M NaCl at pH = 7.59.

0.7 NaCl (pH = 7.58; pH' = 7.59)

Time (hours)	[Ni]eq (mol/L)	Γ[Ni]ad (mol/m^2)	[Ni]des (mol/L)	Γ[Ni]ad'(mol/m^2)	Desorption Ratio
60.58	3.8E-06	9.8E-08	4.0E-007	7.8E-007	0.20
60.58	7.0E-06	1.5E-07	5.1E-007	9.8E-007	0.38
60.79	1.6E-05	2.1E-07	4.6E-007	8.8E-007	0.59
60.79	2.1E-05	6.9E-07	5.2E-007	1.0E-006	0.85
61.15	3.7E-05	6.4E-07	1.2E-006	2.3E-006	0.64
61.15	4.7E-05	1.2E-06	1.0E-006	1.9E-006	0.85
61.24	6.9E-05	2.2E-06	1.1E-006	2.2E-006	0.90
61.24	7.9E-05	1.8E-06	1.4E-006	2.6E-006	0.86

pH = pH value at the onset of the experiment
pH' = pH value by the end of the experiment
Time = time period over which desorption was allowed to proceed
$[Ni]_{eq}$ = total Ni concentration present in solution by the end of the adsorption experiment
$\Gamma[Ni]_{ad}$ = Ni adsorption density
$[Ni]_{eq'}$ = total Ni concentration present in solution by the end of the desorption experiment
$\Gamma[Ni]_{ad'}$ = Ni adsorption density after Ni desorption
Desorption ratio = $\Gamma[Ni]_{ad} / \Gamma[Ni]_{ad'}$

Appendix 5.2- The table below represents a compilation of the data obtained from adsorption isotherm experiments coupled with data obtained from desorption experiments carried out in 0.1M NaCl at pH = 7.98.

0.1 NaCl (pH = 8.0; pH' = 7.98)

Time (hours)	[Ni]eq (mol/L)	Γ[Ni]ad (mol/m^2)	[Ni]eq' (mol/L)	Γ[Ni]ad'(mol/m^2)	Desorption Ratio
50.35	2.2E-05	3.1E-007	9.4E-005	1.8E-007	0.59
50.35	3.7E-05	7.7E-007	2.9E-004	5.8E-007	0.75
50.75	5.7E-05	1.5E-006	5.1E-004	1.0E-006	0.64
50.75	8.5E-05	2.2E-006	9.6E-004	1.8E-006	0.85
51.12	1.2E-04	2.4E-006	1.2E-003	2.3E-006	0.97
51.12	1.7E-04	2.4E-006	1.0E-003	2.0E-006	0.86

pH = pH value at the onset of the experiment
pH' = pH value by the end of the experiment
Time = time period over which desorption was allowed to proceed
$[Ni]_{eq}$ = total Ni concentration present in solution by the end of the adsorption experiment
$\Gamma[Ni]_{ad}$ = Ni adsorption density
$[Ni]_{eq'}$ = total Ni concentration present in solution by the end of the desorption experiment
$\Gamma[Ni]_{ad'}$ = Ni adsorption density after Ni desorption
Desorption ratio = $\Gamma[Ni]_{ad} / \Gamma[Ni]_{ad'}$

Appendix 5.3- The table below represents a compilation of the data obtained from adsorption isotherm experiments coupled with data obtained from desorption experiments carried out in 0.7M NaCl at pH = 8.06.

0.7 NaCl (pH = 8.02; pH' = 8.06)

Time (hours)	[Ni]eq (mol/L)	Γ[Ni]ad (mol/m^2)	[Ni]eq' (mol/L)	Γ[Ni]ad'(mol/m^2)	Desorption Ratio
55.43	1.1E-005	1.9E-007	8.2E-007	3.9E-008	0.2
55.43	2.2E-005	3.1E-007	1.1E-006	8.4E-008	0.27
55.58	3.7E-005	7.7E-007	1.5E-006	4.8E-007	0.62
55.58	5.7E-005	1.5E-006	1.2E-006	1.3E-006	0.85
5575	8.9E-005	2.2E-006	4.1E-006	1.4E-006	0.64
55.75	1.0E-004	2.4E-006	1.8E-006	2.0E-006	0.85
55.92	1.1E-004	2.4E-006	1.8E-006	2.0E-006	0.85

pH = pH value at the onset of the experiment
pH' = pH value by the end of the experiment
Time = time period over which desorption was allowed to proceed
$[Ni]_{eq}$ = total Ni concentration present in solution by the end of the adsorption experiment
$\Gamma[Ni]_{ad}$ = Ni adsorption density
$[Ni]_{eq'}$ = total Ni concentration present in solution by the end of the desorption experiment
$\Gamma[Ni]_{ad'}$ = Ni adsorption density after Ni desorption
Desorption ratio = $\Gamma[Ni]_{ad} / \Gamma[Ni]_{ad'}$

Appendix 5.4- The table below represents a compilation of the data obtained from adsorption isotherm experiments coupled with data obtained from desorption experiments carried out in 0.1 M NaCl at pH = 8.26.

0.1 NaCl (pH = 8.36; pH' = 8.26)

Time (hours)	[Ni]eq (mol/L)	Γ[Ni]ad (mol/m^2)	[Ni]eq' (mol/L)	Γ[Ni]ad'(mol/m^2)	Desorption Ratio
63.16	2.7E-06	7.2E-08	1.2E-007	4.7E-008	0.65
63.16	8.5E-06	4.5E-07	1.3E-007	4.2E-007	0.94
63.55	2.8E-05	1.0E-07	2.0E-007	6.2E-008	0.61
63.55	3.7E-05	6.8E-07	2.3E-007	6.3E-007	0.94
63.71	5.8E-05	1.2E-06	2.7E-007	1.1E-006	0.96
63.71	6.7E-05	2.2E-06	3.2E-007	2.1E-006	0.97
63.88	7.5E-05	3.8E-06	3.8E-007	3.7E-006	0.98
63.88	1.1E-04	9.2E-07	3.6E-007	8.5E-007	0.92

pH = pH value at the onset of the experiment
pH' = pH value by the end of the experiment
Time = time period over which desorption was allowed to proceed
$[Ni]_{eq}$ = total Ni concentration present in solution by the end of the adsorption experiment
$\Gamma[Ni]_{ad}$ = Ni adsorption density
$[Ni]_{eq'}$ = total Ni concentration present in solution by the end of the desorption experiment
$\Gamma[Ni]_{ad'}$ = Ni adsorption density after Ni desorption
Desorption ratio = $\Gamma[Ni]_{ad} / \Gamma[Ni]_{ad'}$

Appendix 5.5- The table below represents a compilation of the data obtained from adsorption isotherm experiments coupled with data obtained from desorption experiments carried out in 0.7M NaCl at pH = 8.32.

0.7 NaCl (pH = 8.26; pH' = 8.32)

Time (hours)	[Ni]eq (mol/L)	Γ[Ni]ad (mol/m^2)	[Ni]eq' (mol/L)	Γ[Ni]ad'(mol/m^2)	Desorption Ratio
60.4	8.5E-006	1.6E-008	7.7E-006	1.5E-008	0.92
60.4	2.8E-005	1.9E-007	-8.5E-007	3.1E-010	N/A
60.68	3.7E-005	2.0E-007	4.2E-005	8.4E-008	0.42
60.68	5.8E-005	7.6E-007	2.3E-004	4.5E-007	0.59
60.95	6.7E-005	3.3E-007	9.5E-005	1.8E-007	0.56
60.95	7.5E-005	1.0E-006	4.5E-004	8.8E-007	0.87
61.2	1.1E-004	4.2E-006	2.0E-003	3.8E-006	0.92

pH = pH value at the onset of the experiment
pH' = pH value by the end of the experiment
Time = time period over which desorption was allowed to proceed
$[Ni]_{eq}$ = total Ni concentration present in solution by the end of the adsorption experiment
$\Gamma[Ni]_{ad}$ = Ni adsorption density
$[Ni]_{eq'}$ = total Ni concentration present in solution by the end of the desorption experiment
$\Gamma[Ni]_{ad'}$ = Ni adsorption density after Ni desorption
Desorption ratio = $\Gamma[Ni]_{ad} / \Gamma[Ni]_{ad'}$

Appendix 5.6- The table below represents a compilation of the data obtained from adsorption isotherm experiments coupled with data obtained from desorption experiments carried out in 0.1M NaCl at pH = 8.66.

0.1 NaCl (pH = 8.66; pH' = 8.66)

Time (hours)	[Ni]eq (mol/L)	Γ[Ni]ad (mol/m^2)	[Ni]eq' (mol/L)	Γ[Ni]ad'(mol/m^2)	Desorption Ratio
63.15	8.0E-06	1.9E-07	not detectable	1.9E-07	1
63.15	1.4E-05	6.0E-07	not detectable	6.0E-07	1
63.21	2.2E-05	9.0E-07	not detectable	9.0E-07	1
63.21	4.0E-05	2.1E-06	not detectable	2.1E-06	1
63.47	6.5E-05	3.6E-06	not detectable	3.6E-06	1
63.47	8.4E-05	4.0E-06	not detectable	4.0E-06	1
64.05	9.9E-005	4.7E-006	not detectable	4.7E-006	1

pH = pH value at the onset of the experiment
pH' = pH value by the end of the experiment
Time = time period over which desorption was allowed to proceed
$[Ni]_{eq}$ = total Ni concentration present in solution by the end of the adsorption experiment
$\Gamma[Ni]_{ad}$ = Ni adsorption density
$[Ni]_{eq'}$ = total Ni concentration present in solution by the end of the desorption experiment
$\Gamma[Ni]_{ad'}$ = Ni adsorption density after Ni desorption
Desorption ratio = $\Gamma[Ni]_{ad} / \Gamma[Ni]_{ad'}$

Appendix 5.7- The table below represents a compilation of the data obtained from adsorption isotherm experiments coupled with data obtained from desorption experiments carried out in 0.7M NaCl at pH = 8.66.

0.7 NaCl (pH = 8.66; pH' = 8.66)

Time (hours)	[Ni]eq (mol/L)	Γ[Ni]ad (mol/m^2)	[Ni]eq' (mol/L)	Γ[Ni]ad'(mol/m^2)	Desorption Ratio
73.25	1.1E-05	6.8E-07	1.4E-006	4.0E-007	0.59
73.25	1.7E-05	2.0E-06	1.5E-006	1.7E-006	0.85
73.41	2.3E-05	3.5E-06	1.5E-006	3.2E-006	0.92
73.41	2.8E-05	6.4E-06	1.5E-006	6.1E-006	0.95
73.8	9.8E-07	1.2E-05	9.6E-007	1.2E-005	0.99
73.8	9.5E-07	1.7E-05	8.4E-007	1.7E-005	0.99

pH = pH value at the onset of the experiment
pH' = pH value by the end of the experiment
Time = time period over which desorption was allowed to proceed
$[Ni]_{eq}$ = total Ni concentration present in solution by the end of the adsorption experiment
$\Gamma[Ni]_{ad}$ = Ni adsorption density
$[Ni]_{eq'}$ = total Ni concentration present in solution by the end of the desorption experiment
$\Gamma[Ni]_{ad'}$ = Ni adsorption density after Ni desorption
Desorption ratio = $\Gamma[Ni]_{ad} / \Gamma[Ni]_{ad'}$

Appendix 5.8- The table below represents a compilation of the data obtained from adsorption isotherm experiments coupled with data obtained from desorption experiments carried out in 0.1M NaCl at pH = 8.90.

0.1 M NaCl (pH = 8.92; pH' = 8.90)

Time (hours)	[Ni]eq (mol/L)	Γ[Ni]ad (mol/m^2)	[Ni]eq' (mol/L)	Γ[Ni]ad'(mol/m^2)	Desorption Ratio
55.86	4.7E-06	3.6E-07	1.8E-06	1.9E-008	0.05
55.86	7.7E-06	8.2E-07	3.6E-06	1.3E-007	0.16
55.95	1.4E-05	7.7E-07	3.0E-006	1.9E-007	0.25
55.95	2.2E-05	1.7E-06	5.9E-006	5.7E-007	0.33
56.28	2.5E-05	2.8E-06	5.7E-006	1.7E-006	0.61
56.28	2.9E-05	2.7E-06	5.7E-006	1.6E-006	0.59
56.53	3.2E-05	3.4E-06	5.3E-006	2.4E-006	0.70

pH = pH value at the onset of the experiment
pH' = pH value by the end of the experiment
Time = time period over which desorption was allowed to proceed
$[Ni]_{eq}$ = total Ni concentration present in solution by the end of the adsorption experiment
$\Gamma[Ni]_{ad}$ = Ni adsorption density
$[Ni]_{eq'}$ = total Ni concentration present in solution by the end of the desorption experiment
$\Gamma[Ni]_{ad'}$ = Ni adsorption density after Ni desorption
Desorption ratio = $\Gamma[Ni]_{ad} / \Gamma[Ni]_{ad'}$

Appendix 5.9- The table below represents a compilation of the data obtained from adsorption isotherm experiments coupled with data obtained from desorption experiments carried out in 0.7M NaCl at pH = 8.95.

0.7 M NaCl (pH = 8.92; pH' = 8.95)

Time (hours)	$[Ni]_{eq}$ (mol/L)	$\Gamma[Ni]_{ad}$ (mol/m^2)	$[Ni]_{eq'}$ (mol/L)	$\Gamma[Ni]_{ad'}$ (mol/m^2)	Desorption Ratio
47.16	1.4E-05	3.6E-08	1.4E-008	2.8E-008	0.79
47.16	2.2E-05	1.9E-07	5.7E-008	1.1E-007	0.57
47.35	2.5E-05	1.9E-06	5.3E-007	1.0E-006	0.54
47.35	2.9E-05	3.4E-06	1.3E-006	2.5E-006	0.74
47.68	3.2E-05	6.5E-06	7.9E-007	1.5E-006	0.23
47.68	3.3E-05	9.3E-06	1.8E-006	3.4E-006	0.37

pH = pH value at the onset of the experiment
pH' = pH value by the end of the experiment
Time = time period over which desorption was allowed to proceed
$[Ni]_{eq}$ = total Ni concentration present in solution by the end of the adsorption experiment
$\Gamma[Ni]_{ad}$ = Ni adsorption density
$[Ni]_{eq'}$ = total Ni concentration present in solution by the end of the desorption experiment
$\Gamma[Ni]_{ad'}$ = Ni adsorption density after Ni desorption
Desorption ratio = $\Gamma[Ni]_{ad} / \Gamma[Ni]_{ad'}$